DOI: 10.1161/CIRCULATIONAHA.114.013675

Oxidative Stress Activates Endothelial Innate Immunity via Sterol Regulatory Element Binding Protein 2 (SREBP2) Transactivation of MiRNA-92a

Running title: *Chen et al.; Oxidative stress induces miR-92a and inflammasome*

Zhen Chen, PhD[1*]; Liang Wen, MD, PhD[1*]; Marcy Martin[1,2]; Chien-Yi Hsu, MD[3,4]; Longhou Fang, PhD[1]; Feng-Mao Lin, PhD[5]; Ting-Yang Lin[1]; McKenna J. Geary[1]; Gregory Geary, PhD[6]; Yongli Zhao, MD[7]; David A. Johnson, PhD[8], Jaw-Wen Chen, MD[3,4]; Shing-Jong Lin, MD, PhD[3,4]; Shu Chien, MD, PhD[9]; Hsien-Da Huang, PhD[5]; Yury I. Miller, MD, PhD[1]; Po-Hsun Huang, MD, PhD[3,4]; John Y-J. Shyy, PhD[1,8]

[1]Dept of Medicine, School of Medicine, University of California, San Diego, CA; [2]Biochemistry and Molecular Biology Graduate Program, University of California, Riverside, CA; [3]Division of Cardiology, Dept of Medicine, Taipei Veterans General Hospital, Taipei, Taiwan; [4]Cardiovascular Research Center, National Yang-Ming University, Taipei, Taiwan; [5]Institute of Bioinformatics and Systems Biology and Dept of Biological Science and Technology, National Chiao Tung University, Hsin-Chu, Taiwan; [6]Dept of Kinesiology and Health Sciences, California State University, San Bernardino, CA; [7]Cardiovascular Research Center, Medical School, Xi'an Jiaotong University, Xi'an, China; [8]Division of Biomedical Sciences, School of Medicine, University of California, Riverside, CA; [9]Dept of Bioengineering, University of California, San Diego, CA

* share co-first authorship

Address for Correspondence:

John Y-J. Shyy, PhD
Dept of Medicine, School of Medicine
University of California, San Diego
9500 Gilman Dr.
La Jolla, CA 92093
Tel: 858-534-3736
Fax: 858-822-3027
E-mail: jshyy@ucsd.edu

Zhen Chen, PhD
Dept of Medicine, School of Medicine
University of California, San Diego
9500 Gilman Dr.
La Jolla, CA 92093
Tel: 858-534-2878
Fax: 858-822-3027
E-mail: zchen@ucsd.edu

Journal Subject Codes: Vascular biology:[95] Endothelium/vascular type/nitric oxide, Atherosclerosis:[138] Cell signaling/signal transduction, Atherosclerosis:[143] Gene regulation

DOI: 10.1161/CIRCULATIONAHA.114.013675

Abstract

***Background*—**Oxidative stress activates endothelial innate immunity and disrupts endothelial functions, including eNOS-derived NO bioavailability. Here, we postulated that oxidative stress induces sterol regulatory element binding protein 2 (SREBP2) and microRNA-92a (miR-92a), which in turn activate endothelial innate immune response, leading to dysfunctional endothelium.

***Methods and Results*—**Using cultured endothelial cells (ECs) challenged by diverse oxidative stresses, hypercholesterolemic zebrafish, and Ang II-infused or aged mice, we demonstrated that SREBP2 transactivation of microRNA-92a (miR-92a) is oxidative stress-inducible. The SREBP2-induced miR-92a targets key molecules in endothelial homeostasis, including Sirtuin 1, Krüppel-like factor 2 (KLF2), and KLF4, leading to NOD-like receptor family, pyrin domain-containing 3 (NLRP3) inflammasome activation and eNOS inhibition. In EC-specific SREBP2 transgenic mice, locked nucleic acid (LNA)-modified antisense miR-92a (LNA-92a) attenuates inflammasome, improves vasodilation, and ameliorates Ang II-induced and aging-related atherogenesis. In patients with coronary artery disease, the level of circulating miR-92a is inversely correlated with EC-dependent, flow-mediated vasodilation and is positively correlated with serum level of IL-1β.

***Conclusions*—**Our findings suggest that SREBP2-miR-92a-inflammasome exacerbates endothelial dysfunction during oxidative stress. Identification of this mechanism may help in diagnosis and/or treatment of disorders associated with oxidative stress, innate immune activation, and endothelial dysfunction.

Key words: endothelial cell, microRNA, sterol regulatory element binding proteins, inflammation, oxidative stress, inflammasome, endothelial dysfunction

DOI: 10.1161/CIRCULATIONAHA.114.013675

Introduction

Oxidative stress, imposed by pathophysiological conditions such as hypertension, hyperlipidemia, and aging, triggers inflammatory responses of vascular endothelial cells (ECs). Although not viewed as typical immunogenic cells, ECs are suggested to be sentinel cells that detect danger signals, initiate innate immune responses, produce pro-inflammatory cytokines and chemokines, and recruit immune cells.[1,2] Such increase in the endothelial innate immunity has emerged as an important mechanism underlying the interplay among oxidative stress, inflammation, and endothelial dysfunction.

Sterol regulatory element-binding proteins (SREBPs) are master regulators in cholesterol and lipid homeostasis.[3] Decreases in the intracellular level of fatty acid or cholesterol activate SREBP1 or SREBP2 through a 2-step proteolytic cleavage, and the resulting mature N-terminal SREBPs transactivate genes involved in cholesterol and lipid synthesis. Recently, SREBPs have been implicated in innate immune responses in vascular cells, due to their regulation of inflammasomes, the intracellular multi-protein complexes mediating the activation of caspase-1 and subsequent maturation of interleukin 1β (IL-1β)/interleukin 18 (IL-18).[4] Im *et al*. showed that SREBP1 activates the NOD-like receptor family, pyrin domain-containing 1 (NLRP1) inflammasome in LPS-stimulated macrophages[5] and we reported that SREBP2 activates NLRP3 inflammasome in ECs under disturbed flow.[6] Importantly, ectopic expression of SREBP2 in murine endothelium is sufficient to aggravate atherosclerosis, partially through the increased caspase-1-dependent IL-1β production, which suggests a primary role of EC innate immunity in atherogenesis.[6] In human aortic sections, activated SREBPs are observed in macrophages and ECs in the atherosclerotic lesions.[7] Although these studies suggest that SREBPs are critical regulators in vascular innate immunity, the upstream stress stimuli that induce or activate

SREBPs and the SREBP downstream targets that disturb EC homeostasis are largely unexplored.

Stimuli such as disturbed flow and oxidized lipids that impose oxidative stress in ECs increase SREBP levels.[6,8,9] They also induce microRNA-92a (miR-92a), a crucial miRNA that inhibits EC angiogenesis and impairs EC function.[10-12] At the molecular level, miR-92a targets Krüppel-like factor 2 (KLF2), KLF4, and possibly Sirtuin 1 (SIRT1), all of which are tightly associated with redox balance, eNOS-derived NO bioavailability, and the inflammatory state.[10,12-14] In regards to endothelial innate immune response, KLF2, KLF4, and SIRT1 suppress the production or antagonize the effect of IL-1β.[15-17] In terms of translational implications, administration of locked nucleic acid (LNA)-modified antisense miR-92a (LNA-92a) prevents ischemic injury in pigs and ameliorates hyperlipidemia-induced atherosclerosis in mice.[11,18] Despite the involvement of miR-92a in EC dysfunction, the molecular mechanism underlying stress-induction of miR-92a in ECs and its link to endothelial innate immunity is unclear.

Given the common stimuli (e.g. disturbed flow and oxidized lipids) and convergent functional consequences (i.e. endothelial inflammation and dysfunction) of SREBP2 and miR-92a, we postulated that oxidative stress induces SREBP2 and miR-92a, which in turn activate innate immune response, leading to dysfunctional endothelium. Here, we demonstrate that the SREBP2 transactivation of miR-92a is a ubiquitous response to oxidative stress. Downstream, this redox-sensitive pathway decreases the expression of anti-inflammatory genes, including SIRT1, KLF2, and KLF4, thus resulting in increased inflammasome and impaired eNOS-NO bioavailability. Furthermore, studies of zebrafish, mouse, and human samples suggest an inverse correlation between miR-92a level and functional endothelium.

DOI: 10.1161/CIRCULATIONAHA.114.013675

Methods

Crosslinking immunoprecipitation (CLIP) and chromatin immunoprecipitation (ChIP)

For CLIP, HUVECs were irradiated with UV light at 400 mJ/cm^2 to crosslink RNA and proteins. Cells were then lysed in a buffer containing 50 mM Tris-HCl, pH 7.5, 150 mM NaCl, 0.1% NP-40, 1 mM EDTA, and 100 U/μl RNase inhibitor. The lysates were incubated with protein G Dynabeads conjugated with anti-AGO2 (clone 4G8; Wako Chemicals) at 4°C overnight. Mouse IgG was used as an isotype control. The immunoprecipitated RNAs were then extracted with Trizol. For ChIP, HUVECs were treated with 0.75% formaldehyde for 20 minutes at room temperature. After sonication, the SREBP2-bound chromatin was immunoprecipitated by rabbit anti-SREBP2(N) (Abcam) conjugated to protein A Dynabeads. Protein and RNA were degraded by proteinase K and RNase A, respectively. The purified chromatin DNA was then used as the template for qPCR. As an isotype control, rabbit IgG was used in ChIP.

Flow cytometry and NO bioavailability assay

Active caspase-1 was detected in living ECs with use of the Fluorescent Labeled Inhibitor of Caspases (FLICA) caspase-1 assay kit (ImmunoChemistry Technologies). FLICA-FAM-YVAD-FMK is a cell-permeable, non-toxic fluorochrome inhibitor of caspase-1 that interacts with the enzymatic-reactive center of activated caspase-1 via the YVAD recognition sequence, thus forming a covalent thioether adduct with the enzyme through the FMK moiety. The resulting green fluorescence is a direct measure of caspase-1 activity, which was analyzed by FACS with 488-nm excitation and 530-nm emission. NO was detected as the accumulated nitrite/nitrate, the stable breakdown product of NO, in cell culture media by use of a nitrate/nitrite fluorometric assay (Cayman Chemicals).

In vivo Ang II infusion and administration of LNA

All animal experiments were approved by UCSD IACUC. EC-SREBP2(N)-Tg and ApoE$^{-/-}$/EC-SREBP2(N)-Tg mice were created as described.[6] LNAs were designed and synthesized by Exiqon Inc, with the following sequences 5'-AGGCCGGGACAAGTGCAAT-3' (LNA-92a) and 5'-TAACACGTCTATACGCCCA-3' (LNA-control). Male ApoE$^{-/-}$/EC-SREBP2(N)-Tg and their age- and gender- matched ApoE$^{-/-}$ littermates were used for the Ang II infusion and LNA injection. As illustrated in **Supplemental Figure 1**, one week before Ang II infusion, mice received tail-vein injections of LNA-control or LNA-92a at 16 mg/kg BW, a dose that effectively inhibits miR-92a expression.[11] Osmotic minipumps (Alzet, Model 1004) filled with Ang II solution were implanted subcutaneously into the dorsal side of mice. Ang II was released at 1 □g/kg/min for 28-day. The second dose of LNA was given 10 days after the minipump implantation. The animals were sacrificed at the end of 28-day post minipump implantation.

IK17-EGFP Tg zebrafish

Tg(hsp70l:Hsa.IK17-EGFP) zebrafish with temperature-inducible expression of the EGFP-labeled single-chain human mAb IK17 (i.e. IK17-EGFP) was described.[19] IK17-EGFP is driven by hsp70 and hence can be induced by heat shock at 37°C. Zebrafish larvae at 5-day post fertilization were fed a normal diet or high-cholesterol diet (HCD) containing 4% cholesterol for 4-week. One group of HCD-fed fish were subjected to heat shock (1 hour at 37°C) once every 3-day to maintain IK17-EGFP expression during the feeding period. The expression of IK17-EGFP was confirmed by microscopy (excitation at 488 nm).

Clinical samples, measurement of circulating miR-92a, IL-1β and flow-mediated dilation (FMD)

All clinical samples were obtained at Taipei Veterans General Hospital, with informed consent

and IRB approval (protocol number: 2014-02-002A). The baseline characteristics of patients are summarized in **Supplemental Table 1**. Sera were collected after an 8-hour overnight fast. Circulating miR-92a level was measured as described.[20] IL-1β level was assessed by ELISA (Human IL-1β Quantikine ELISA Kit, R&D Systems). Each standard and plasma sample was analyzed twice, and the mean value was used in all subsequent analyses. Endothelium-dependent FMD was assessed by use of a 7.5-MHz linear array transducer (Hewlett-Packard Sonos 5500) to scan the brachial artery in longitudinal sections, as described[21] (Supplemental methods).

Statistical analysis

Data from *in vitro* experiments are expressed as mean±SD from at least 3 independent experiments, unless otherwise noted. Data from *in vivo* studies are expressed as mean±SEM. Two groups were compared by Student's *t* test. Differences among multiple groups were evaluated by ANOVA followed by the Bonferroni post hoc test for equal sample sizes or Tukey-Kramer test for unequal sample sizes. Correlational analyses were performed using Spearman's correlation after determining the (non-)normal distribution of the data. Values of $p < 0.05$ was considered statistically significant.

Supplemental methods

Additional experimental procedures are described in "Supplemental Methods".

Results

SREBP2 and miR-92a are induced by oxidative stress in ECs

We first sought to test whether SREBP2 and miR-92a are induced by H_2O_2, Ang II, and oxidized LDL (ox-LDL), all of which directly or indirectly increase ROS in ECs to result in inflammatory

responses. All 3 stimuli induced and activated SREBP2 in HUVECs, as evidenced by increased level of the SREBP2 precursor, as well as mature form of SREBP2 [i.e., SREBP2(N)] (**Figure 1A**). The activation of SREBP2 was associated with induction of SREBP2 transactivation targets such as LDLR and squalene synthase (**Figure 1B**). Notably, H_2O_2, Ang II, and ox-LDL also dose-dependently increased the level of miR-92a (**Figure 1, C-E**). Pretreatment with the ROS scavenger EUK-134, a catalase/SOD mimetic,[22] attenuated the H_2O_2-, Ang II-, and ox-LDL-induced SREBP2 and miR-92a levels (**Figure 1, F-H**). These results indicate that SREBP2 and miR-92a are induced by oxidative stress in ECs.

SREBP2 transactivates miR-92a under oxidative stress

To examine whether SREBP2 transactivates miR-92a in response to oxidative stress, we performed bioinformatics analysis for putative sterol regulatory elements (SREs) in the promoter region of the miR-17-92 cluster. We found 8 SREs in the promoter region of the human miR-17-92 cluster, which are conserved in the mouse gene (**Figure 2A**; **Supplemental Table 2**). To validate this *in silico* prediction, we overexpressed the active/mature form of SREBP2, i.e. SREBP2(N) in ECs, which increased the level of miR-92a (**Figure 2B**). Conversely, knockdown of SREBP2 with siRNA inhibited H_2O_2-induced miR-92a (**Figure 2C**). To demonstrate enhanced transactivation of miR-92a by SREBP2 under oxidative stress, we performed ChIP assays to assess the direct binding of SREBP2 to SREs in the miR-17-92 promoter. H_2O_2 treatment of ECs or ectopic expression of SREBP2(N) in ECs, mimicking SREBP2 induction by oxidative stress, substantially enriched SREBP2(N) binding to segments of miR-92a promoter containing the predicted SREs (**Figure 2, D and E**). Thus, oxidative stress-activated/induced SREBP2 transactivates miR-92a.

Oxidative stress-induced miR-92a increases endothelial innate immunity

Recent findings suggest that SREBP induction or activation increases innate immunity, specifically, via NLRP3 inflammasome activation in ECs and macrophages.[5,6] Because oxidative stress activates SREBP2-miR-92a (**Figures 1 and 2**), we examined whether oxidative stress activates inflammasome, and if so, the role of miR-92a in this innate immune response in ECs. H_2O_2, Ang II, and ox-LDL all increased the cleaved form of caspase-1 and IL-1β, hallmarks of inflammasome activation (**Figure 3**, **A and B**). Importantly, pre-miR-92a, mimicking miR-92a induction by SREBP2, also increased the cleavage of caspase-1 and IL-1β (**Figure 3, C and D**). Conversely, transfecting ECs with anti-miR-92a blocked these inflammasome-related events in H_2O_2-stimulated ECs (**Figure 3, E and F**). These results were further confirmed by using flow cytometry to detect the active caspase-1 in living cells (**Figure 3, G and H**). Therefore, the SREBP2-miR-92a axis contributes to oxidative stress-induction of the endothelial innate immune response, as evidenced by inflammasome activation.

miR-92a targeting SIRT1, KLF2, and KLF4 increases endothelial innate immunity but decreases NO bioavailability

Oxidative stress-induced miR-92a should target KLF2, KLF4 (previously validated)[12,14] and SIRT1 mRNAs (previously predicted)[10], to result in increased IL-1β production but decreased NO bioavailability. Thus, we first verified the direct targeting of the SIRT1 3' untranslated region (3'UTR) by miR-92a (**Supplemental Figure 2A**). Using a luciferase reporter containing SIRT1 3'UTR or its mutant, we confirmed that miR-92a directly targets SIRT1 mRNA (**Supplemental Figure 2, B and C**), which agrees with pre-miR-92a-decreased levels of SIRT1 mRNA, protein, and activity (revealed by increased acetylation of SIRT1 substrates p53 and NF-κB) (**Supplemental Figure 2, D and E**).

We next assessed whether oxidative stress increases the recruitment of miR-92a and its

targeted SIRT1, KLF2, and KLF4 mRNAs to Argonaute (AGO)-mediated-miRNA-induced silencing complex (miRISC) in ECs. H_2O_2, Ang II, or ox-LDL treatment increased the association of miR-92a, SIRT1, KLF2, and KLF4 mRNAs with miRISC in ECs (**Figure 4, A-C**). As a control, H_2O_2 did not change the association of miR-92a with non-specific RNAs such as α-tubulin mRNA and 5S ribosomal RNA (5S rRNA) (data not shown). In agreement with the co-enrichment of miR-92a and its target mRNAs in miRISC, these stimuli decreased the luciferase activity in ECs transfected with luciferase reporters conjugated to the 3'UTR of SIRT1, KLF2, and KLF4 containing the miR-92a binding/responsive elements (MREs) as compared with untreated cells. This reduction of luciferase activity was restored by co-transfection of anti-miR-92a (**Figure 4, D-F**). Functionally, anti-miR-92a ameliorated the H_2O_2-decreased mRNA and protein levels of SIRT1, KLF2, and KLF4 as well as eNOS expression and activity (**Figure 4, G-I**). The suppression of SIRT1, KLF2, and KLF4 by H_2O_2 was mimicked by SREBP2(N) overexpression, whereas co-transfection with anti-miR-92a restored the levels of SIRT1, KLF2, and KLF4 (**Figure 4J**). Furthermore, the effect of ectopic expression of SIRT1, KLF2, and KLF4 was similar to anti-miR-92a in reversing the H_2O_2-induced EC inflammation (i.e., caspase-1 activation and IL-1β production) and H_2O_2-impaired NO bioavailability (**Figure 4, K and L**). Collectively, oxidative stress induction of SREBP2-miR-92a and the subsequent SIRT1, KLF2, and KLF4 targeting increases endothelial innate immunity and impairs eNOS-NO bioavailability, two key features of endothelial dysfunction.

SREBP2 induction of miR-92a leads to impaired EC functions in the vessel wall

We next examined whether miR-92a is oxidative stress-inducible in the vessel wall *in vivo* in mouse and zebrafish models. The aortic miR-92a level was higher in the Ang II-infused C57BL6 mice than normotensive controls (**Figure 5A**). Consistent with increased oxidative

stress in the aging vessel,[23,24] the miR-92a level in the aortas was also higher in 12- than 3-month-old C57BL6 mice (**Figure 5B**). We also used a hypercholesterolemic zebrafish model with accelerated vascular accumulation of oxidized lipids with enhanced oxidation-specific epitopes (OSEs).[19,25] Four-week HCD significantly increased miR-92a level in the trunks, where major blood vessels are located. This induction was substantially inhibited in zebrafish expressing IK17, a human mAb against malondialdehyde-LDL and ox-LDL[19,26] (**Figure 5, C and D**). Thus, miR-92a was also induced in the zebrafish in an oxidative stress-dependent manner. To examine whether SREBP2 increases miR-92a in the endothelium *in vivo*, we assessed the miR-92a level in intima isolated from EC-SREBP2(N)-Tg mice with the active form of SREBP2 overexpressed only in the endothelium.[6] Ectopic expression of SREBP2(N) increased the miR-92a level and decreased mRNA level of SIRT1, KLF2, KLF4, and eNOS in the intima (**Figure 5E**). Furthermore, an endothelial innate immune response was induced, as evidenced by increased IL-1β mRNAs level in EC-SREBP2(N)-Tg mice (**Figure 5E**). Consistent with the reduced eNOS expression, flow-mediated vasodilation, a hallmark of endothelial dysfunction was attenuated (**Supplemental Figure 3**). To address whether miR-92a mediates the detrimental effects of SREBP2 in the vessel wall, we inhibited miR-92a with LNA in the carotid arteries of EC-SREBP2(N)-Tg mice. While miR-92a was significantly inhibited by LNA, the mRNA levels of SIRT1, KLF2, KLF4, and eNOS were substantially increased and that of IL-1β decreased in mice receiving LNA-92a as compared with control LNA (**Figure 5F**). Functionally, LNA-92a administration improved the flow-mediated vasoreactivity (**Figure 5G**).

To evaluate the detrimental effect of the SREBP2-miR-92a pathway at the disease level, we used a model of EC-SREBP2(N)-Tg in an ApoE$^{-/-}$ background treated with Ang II (1 μg/min/kg). With a regular diet, Ang II infusion accelerates atherosclerosis.[27] Thus, the etiology

of atherosclerosis in this model is due mainly to the oxidative stress-induced endothelial dysfunction rather than diet-induced hyperlipidemia. The experimental design is outlined in **Supplemental Figure 1**, and the efficacy of LNA-92a was confirmed by the decreased miR-92a but increased mRNA levels of miR-92a targets, i.e., SIRT1, KLF2, and KLF4, as well as eNOS (**Supplemental Figure 4A**). Noticeably, atherosclerosis, including overall lesion size and that in the aortic arch, was reduced in mice treated with LNA-92a as compared with control LNA. Furthermore, the inhibitory effect of LNA-92a on atherosclerosis was apparent in both 3- and 12-month-old animals (**Figure 6, A and B**, **Supplemental Figure 4, B and C**). Lung ECs from LNA-92a-treated mice showed decreased inflammasome activity, as indicated by the decreased expression and cleavage of caspase-1 (**Figure 6C**). The miR-92a level in $CD31^+$ microparticles (MPs) collected from sera was higher in Ang II-challenged $ApoE^{-/-}$/EC-SREBP2(N) mice than their $ApoE^{-/-}$ littermates (**Figure 6D**), which suggests that the SREBP2-induced miR-92a in the endothelium was released into the circulation.

miR-92a level is inversely correlated with EC function in patients

To investigate whether circulating miR-92a level is associated with EC function in human patients, we assessed the serum miR-92a level in relation to FMD, the clinical readout for endothelial function.[28] The circulating level of miR-92a was indeed inversely correlated with FMD in 85 patients with diagnosed stable coronary artery disease (CAD) (**Figure 7A**). Conversely, the levels of miR-92a and IL-1β were positively correlated in these patients (**Figure 7B**). Furthermore, the level of circulating miR-92a was positively correlated with miR-92a abundance in the $CD31^+$ MPs (**Figure 7C**), which suggests that miR-92a in circulation in part originats from the endothelium. Therefore, the serum level of miR-92a could indicate endothelial dysfunction and innate immunity under certain cardiovascular events.

Discussion

Here, we demonstrate that oxidative stress activates the endothelial innate immune response by inducing SREBP2-miR-92a. This finding presents a novel function of SREBP2 in addition to its canonical role in cholesterol synthesis and uptake. The induction of this pathway is a common response of ECs to disturbed flow, H_2O_2, Ang II, ox-LDL, and oxidized palmitoyl-arachidonylphosphatidyl choline (ox-PAPC), all of which cause oxidative stress[6,12] (**Figure 1**, and **Supplemental Figure 5**). This response is attenuated when ECs are pretreated with the ROS scavengers SOD/catalase mimetic EUK-134 or cell-permeable SOD (**Figure 1**, **Supplemental Figure 5**), which suggests that the SREBP2-miR-92a pathway is redox-sensitive. *In vivo*, miR-92a is induced in the mouse aorta with increased oxidative stress from Ang II infusion or aging (**Figure 5, A and B**). Similarly, miR-92a is induced in zebrafish by HCD (**Figure 5C**). Because IK17 antagonizes ox-LDL[19,29], the IK17 inhibition of miR-92a further indicates that oxidized lipids and lipoproteins likely induce miR-92a in zebrafish. Together, these *in vitro* and *in vivo* findings strongly suggest that oxidative stress-induced miR-92a is a conserved mechanism among vertebrates. Consistent with this conclusion is the observation that miR-17-92 promoters from human, mouse, and zebrafish all contain multiple putative SREs (**Supplemental Tables 2 and 3**). Intriguingly, when ECs are supplemented with 25-hydroxycholesterol (25-HC) which blocks the canonical cholesterol-sensing pathway, ox-PAPC and disturbed flow are still able to activate SREBP2[3] (**Supplemental Figure 5C**). Thus, oxidative stress induction of miR-92a via SREBP2 differs from miR-33 induction, which responds to sterol depletion.[30] As an SREBP2 intronic miRNA, miR-33a targets the cholesterol transporters ABCA1 and ABCG1 for restoration of cellular cholesterol homeostasis.[30] However,

miR-92a downregulates KLF2, KLF4, and SIRT1 to affect endothelial innate immunity and function. Thus, the redox-sensitive SREBP2, by transactivating miR-92a, mediates the innate immune response in ECs under oxidative stress (**Summarized in Figure 7D**). Because the endothelium does not readily accumulate lipid and cholesterol, these results suggest that the major functional relevance of oxidative stress-induction of SREBP2 in ECs is increased innate immunity rather than cholesterol synthesis, uptake, and storage.

The miR-17-92 cluster is upregulated by c-Myc and NF-κB in cancer cells, fibroblasts, and epithelial cells.[31,32] Although STAT3 regulates miR-92a in ECs,[11] whether STAT3 directly transactivates miR-92a is unknown. Given that (a) NF-κB upregulates SREBP2,[33] (b) STAT3 crosstalks with NF-κB,[34] and (c) SREBP2 and c-Myc are both basic helix-loop-helix transcription factors and likely share transactivating targets that contain E-box in their promoter regions,[35] SREBP2 is likely involved in a network regulating miR-92a. Indeed, the H_2O_2-induced miR-92a is attenuated in ECs if RelA (i.e., NF-κB p65 subunit) or c-Myc has been knocked down (**Supplemental Figure 6A**). Because toll-like receptors (TLRs) are key mediators in innate immunity and most, if not all TLRs are expressed in ECs, we have also examined the TLR pathway involved in the oxidative stress-induced miR-92a. When we inhibited myeloid differentiation factor 88 (Myd88), a common signaling adaptor downstream of TLRs except TLR3, the ox-LDL-induced miR-92a was suppressed (**Supplemental Figure 6B**). In line with this, Myd88 inhibition also attenuated the activation and induction of SREBP2 in LPS-stimulated macrophages and the consequent foam cell formation.[33] Therefore, SREBP2-miR-92a may act as a critical nexus linking oxidative stress and endothelial innate immune response and subsequent inflammation.

Most, if not all, oxidative insults suppress SIRT1, KLF2, and KLF4, as well as uncouple

eNOS in ECs.[14,36-38] Because of the positive effect of SIRT1, KLF2, and KLF4 on the NO bioavailability, the finding that SREBP2-miR-92a suppresses the expression of SIRT1, KLF2, and KLF4 (**Figures 4, 5**) reveals a post-transcriptional mechanism by which oxidative stress diminishes NO bioavailability, thus resulting in endothelial dysfunction. Another new finding is the SREBP2-miR-92a induction of inflammasome in ECs (**Figure 3**). Given that SIRT1 deacetylates and inhibits NF-κB[39] (**Supplemental Figure 2**) and that KLF2 and KLF4 suppress both IL-1β expression and IL-1β-mediated inflammatory responses,[15,16] miR-92a-induced innate immune responses (i.e., inflammasome and IL-1β induction) likely also involve targeting SIRT1, KLF2, and KLF4. Indeed, ectopic expression of these genes reversed H_2O_2-stimulated inflammasome activation (**Figure 4K**). Notably, SIRT1 can deacetylate and inhibit SREBP2.[40] Hence, the miR-92a suppression of SIRT1 would further potentiate SREBP2 and inflammasome under oxidative stress. Interestingly, activated caspase-1 proteolytically cleaves not only pro-IL-1β but also SIRT1.[41] While increasing mature IL-1β production and decreasing the level of SIRT1, the oxidative stress-induced miR-92a may provoke a vicious loop of innate immune responses in ECs via inflammasome-dependent activation of caspase-1.

Within the pathophysiologic context, 3 factors would contribute to increased vascular oxidative stress in ApoE$^{-/-}$/EC-SREBP2(N)-Tg mice receiving Ang II (**Figure 6**). First, Ang II accelerates atherogenesis in ApoE$^{-/-}$ mice with increased oxidative stress without altering the lipid profile.[27] Second, ectopic expression of SREBP2(N) in the endothelium increases miR-92a level (**Figure 5C**), which enhances the innate immune response in the intima,[3] independent of other immuno-sensitive cells. Third, aging is an independent factor contributing to increased oxidative stress in the vessel wall.[23] Noticeably, either in LNA-control or LNA-92a group, aging still aggravates atherosclerotic lesion area (**Figure 6, A and B**; **Supplemental Figure 4B**). This

observation suggests that part of the atherosclerotic process in adulthood is less dependent on miR-92a. Because atherogenesis is a complex and multi-factorial process, the aging-induced SREBP2-miR-92a may still be involved in atherosclerosis. Indeed, both SREBP2 and miR-92a levels are increased in the aortas of 12-month-old mice relative to 3-month-old mice (**Figure 5B**, **Supplemental Figure 7**). Thus, we could not rule out the possibility that Ang II may induce higher level of miR-92a in 12 month-old mice, which may require higher degree of miR-92a inhibition to ameliorate the lesion development. In terms of the therapeutic potential of targeting miR-92a in treating cardiovascular impairments, Bonauer *et al* demonstrated that antagomiR-92a significantly improves reperfusion in an ischemic hindlimb model;[10] Hinkel *et al* showed that LNA-92a reduces infarct size and preserves cardiac function in a porcine ischemia/reperfusion model;[18] and Loyer *et al*. found that LNA-92a attenuates atherogenesis in hypercholesterolemic LDLR$^{-/-}$ mice.[11] These therapeutic effects involving miR-92a suppression are probably associated with ameliorated endothelial inflammation and dysfunction. To this end, we observed a pleiotropic effect of LNA-miR-92a in decreasing blood pressure and incidence of aneurysms (data not shown) for which endothelial dysfunction is an independent risk factor.

The increase in miR-92a level in CD31^{+} MPs from ApoE$^{-/-}$/EC-SREBP2(N) mouse sera suggests that miR-92a is released from the endothelium into the circulation under SREBP2 activation (**Figure 6D**). This mechanism is likely common to the human vasculature and is supported by the positive correlation between the miR-92a level in CD31^{+} MPs and circulation (**Figure 7C**). Such an increase could be due, in part, to the increase in EC-derived MPs under pathophysiological conditions,[42] and/or to the augmentation of miR-92a packaged into MPs resulting from increased miR-92a level in ECs. Although the mechanism for EC miR-92a secretion into the circulation via MPs remains to be determined, the translational relevance of

this data is demonstrated by the finding that the circulating miR-92a level is inversely correlated with FMD, a clinical readout of EC-dependent NO bioavailability, and positively correlated with IL-1β, the end-product of inflammasome activation (**Figure 7, A and B**). Because IL-1β can be largely produced by myeloid cells, we propose that oxidative stress-induced miR-92a increases endothelial innate immune response, which predisposes the endothelium to other detrimental factors, including the macrophages-mediated inflammatory response. Thus, the positive correlation between circulating miR-92a and serum IL-1β levels in patients with stable CAD suggests that miR-92a is indicative of vascular inflammation. In line with this, we also observed a significant positive correlation between the circulating miR-92a level with that of high-sensitivity C-reactive protein (hs-CRP), the marker of systemic inflammation in the same group of patients (R=0.502, p<0.001, data not shown). Because of the endothelium-derived nature of miR-92a,[11,43] assessment of circulating miR-92a, in conjunction with CRP may provide further insight into cardiovascular diseases that are initiated from or highly associated with endothelial dysfunction.

Acknowledgments: We thank Dr. Yun Fang (Department of Medicine, University of Chicago) for generously sharing the Luc-KLF4-MRE plasmid, Dr. Sotirios Tsimikas (Department of Medicine, UCSD) for his useful comments, Drs. Jian Kang and Soo Mun Ngoi (Department of Medicine, UCSD) for technical assistance, and Dr. Traci Marin (Department of Cardiopulmonary Sciences, Loma Linda University) for consultation on statistics.

Funding Sources: This work was supported in part by NIH research grants R01HL89940 and R01HL105318 (JS); R01HL106579 and R01HL108735 (JS, SC); K99HL122368 (ZC); R01HL093767 (to YM); and Taiwan Ministry of Science and Technology I-RiCE Program NSC 102-2911-I-009-101 (HH, SL, JC, PH).

Conflict of Interest Disclosures: None.

References:

1. Bell E. Innate Immunity Endothelial Cells as Sentinels. *Nat Rev Immunol*. 2009;9:532-532.

2. Mai J, Virtue A, Shen J, Wang H, Yang XF. An evolving new paradigm: endothelial cells--conditional innate immune cells. *J Hematol Oncol*. 2013;6:61.

3. Horton JD, Goldstein JL, Brown MS. SREBPs: activators of the complete program of cholesterol and fatty acid synthesis in the liver. *J Clin Invest*. 2002;109:1125-1131.

4. Martinon F, Burns K, Tschopp J. The inflammasome: a molecular platform triggering activation of inflammatory caspases and processing of proIL-beta. *Mol Cell*. 2002;10:417-426.

5. Im SS, Yousef L, Blaschitz C, Liu JZ, Edwards RA, Young SG, Raffatellu M, Osborne TF. Linking lipid metabolism to the innate immune response in macrophages through sterol regulatory element binding protein-1a. *Cell Metab*. 2011;13:540-549.

6. Xiao H, Lu M, Lin TY, Chen Z, Chen G, Wang WC, Marin T, Shentu TP, Wen L, Gongol B, Sun W, Liang X, Chen J, Huang HD, Pedra JH, Johnson DA, Shyy JY. Sterol regulatory element binding protein 2 activation of NLRP3 inflammasome in endothelium mediates hemodynamic-induced atherosclerosis susceptibility. *Circulation*. 2013;128:632-642.

7. Li Y, Xu S, Jiang B, Cohen RA, Zang M. Activation of sterol regulatory element binding protein and NLRP3 inflammasome in atherosclerotic lesion development in diabetic pigs. *PLoS One*. 2013;8:e67532.

8. Liu Y, Chen BP, Lu M, Zhu Y, Stemerman MB, Chien S, Shyy JY. Shear stress activation of SREBP1 in endothelial cells is mediated by integrins. *Arterioscler Thromb Vasc Biol*. 2002;22:76-81.

9. Yeh M, Cole AL, Choi J, Liu Y, Tulchinsky D, Qiao JH, Fishbein MC, Dooley AN, Hovnanian T, Mouilleseaux K, Vora DK, Yang WP, Gargalovic P, Kirchgessner T, Shyy JY, Berliner JA. Role for sterol regulatory element-binding protein in activation of endothelial cells by phospholipid oxidation products. *Circ Res*. 2004;95:780-788.

10. Bonauer A, Carmona G, Iwasaki M, Mione M, Koyanagi M, Fischer A, Burchfield J, Fox H, Doebele C, Ohtani K, Chavakis E, Potente M, Tjwa M, Urbich C, Zeiher AM, Dimmeler S. MicroRNA-92a controls angiogenesis and functional recovery of ischemic tissues in mice. *Science*. 2009;324:1710-1713.

11. Loyer X, Potteaux S, Vion AC, Guerin CL, Boulkroun S, Rautou PE, Ramkhelawon B, Esposito B, Dalloz M, Paul JL, Julia P, Maccario J, Boulanger CM, Mallat Z, Tedgui A. Inhibition of microRNA-92a prevents endothelial dysfunction and atherosclerosis in mice. *Circ*

Res. 2014;114:434-443.

12. Wu W, Xiao H, Laguna-Fernandez A, Villarreal G, Jr., Wang KC, Geary GG, Zhang Y, Wang WC, Huang HD, Zhou J, Li YS, Chien S, Garcia-Cardena G, Shyy JY. Flow-Dependent Regulation of Kruppel-Like Factor 2 Is Mediated by MicroRNA-92a. *Circulation*. 2011;124:633-641.

13. Chen Z, Peng IC, Cui X, Li YS, Chien S, Shyy JY. Shear stress, SIRT1, and vascular homeostasis. *Proc Natl Acad Sci U S A*. 2010;107:10268-10273.

14. Fang Y, Davies PF. Site-specific microRNA-92a regulation of Kruppel-like factors 4 and 2 in atherosusceptible endothelium. *Arterioscler Thromb Vasc Biol*. 2012;32:979-987.

15. Liu J, Yang T, Liu Y, Zhang H, Wang K, Liu M, Chen G, Xiao X. Kruppel-like factor 4 inhibits the expression of interleukin-1 beta in lipopolysaccharide-induced RAW264.7 macrophages. *FEBS Lett*. 2012;586:834-840.

16. Parmar KM, Larman HB, Dai G, Zhang Y, Wang ET, Moorthy SN, Kratz JR, Lin Z, Jain MK, Gimbrone MA, Jr., Garcia-Cardena G. Integration of flow-dependent endothelial phenotypes by Kruppel-like factor 2. *J Clin Invest*. 2006;116:49-58.

17. Stein S, Schafer N, Breitenstein A, Besler C, Winnik S, Lohmann C, Heinrich K, Brokopp CE, Handschin C, Landmesser U, Tanner FC, Luscher TF, Matter CM. SIRT1 reduces endothelial activation without affecting vascular function in ApoE-/- mice. *Aging (Albany NY)*. 2010;2:353-360.

18. Hinkel R, Penzkofer D, Zuhlke S, Fischer A, Husada W, Xu QF, Baloch E, van Rooij E, Zeiher AM, Kupatt C, Dimmeler S. Inhibition of microRNA-92a protects against ischemia/reperfusion injury in a large-animal model. *Circulation*. 2013;128:1066-1075.

19. Fang L, Green SR, Baek JS, Lee SH, Ellett F, Deer E, Lieschke GJ, Witztum JL, Tsimikas S, Miller YI. In vivo visualization and attenuation of oxidized lipid accumulation in hypercholesterolemic zebrafish. *J Clin Invest*. 2011;121:4861-4869.

20. Fichtlscherer S, De Rosa S, Fox H, Schwietz T, Fischer A, Liebetrau C, Weber M, Hamm CW, Roxe T, Muller-Ardogan M, Bonauer A, Zeiher AM, Dimmeler S. Circulating microRNAs in patients with coronary artery disease. *Circ Res*. 2010;107:677-684.

21. Huang PH, Chen YH, Chen YL, Wu TC, Chen JW, Lin SJ. Vascular endothelial function and circulating endothelial progenitor cells in patients with cardiac syndrome X. *Heart*. 2007;93:1064-1070.

22. Rong Y, Doctrow SR, Tocco G, Baudry M. EUK-134, a synthetic superoxide dismutase and catalase mimetic, prevents oxidative stress and attenuates kainate-induced neuropathology. *Proc Natl Acad Sci U S A*. 1999;96:9897-9902.

23. Donato AJ, Eskurza I, Silver AE, Levy AS, Pierce GL, Gates PE, Seals DR. Direct evidence of endothelial oxidative stress with aging in humans: relation to impaired endothelium-dependent dilation and upregulation of nuclear factor-kappaB. *Circ Res*. 2007;100:1659-1666.

24. van der Loo B, Labugger R, Skepper JN, Bachschmid M, Kilo J, Powell JM, Palacios-Callender M, Erusalimsky JD, Quaschning T, Malinski T, Gygi D, Ullrich V, Luscher TF. Enhanced peroxynitrite formation is associated with vascular aging. *J Exp Med*. 2000;192:1731-1744.

25. Stoletov K, Fang L, Choi SH, Hartvigsen K, Hansen LF, Hall C, Pattison J, Juliano J, Miller ER, Almazan F, Crosier P, Witztum JL, Klemke RL, Miller YI. Vascular lipid accumulation, lipoprotein oxidation, and macrophage lipid uptake in hypercholesterolemic zebrafish. *Circ Res*. 2009;104:952-960.

26. Shaw PX, Horkko S, Tsimikas S, Chang MK, Palinski W, Silverman GJ, Chen PP, Witztum JL. Human-derived anti-oxidized LDL autoantibody blocks uptake of oxidized LDL by macrophages and localizes to atherosclerotic lesions in vivo. *Arterioscler Thromb Vasc Biol*. 2001;21:1333-1339.

27. Daugherty A, Manning MW, Cassis LA. Angiotensin II promotes atherosclerotic lesions and aneurysms in apolipoprotein E-deficient mice. *J Clin Invest*. 2000;105:1605-1612.

28. Corretti MC, Anderson TJ, Benjamin EJ, Celermajer D, Charbonneau F, Creager MA, Deanfield J, Drexler H, Gerhard-Herman M, Herrington D, Vallance P, Vita J, Vogel R, International Brachial Artery Reactivity Task F. Guidelines for the ultrasound assessment of endothelial-dependent flow-mediated vasodilation of the brachial artery: a report of the International Brachial Artery Reactivity Task Force. *J Am Coll Cardiol*. 2002;39:257-265.

29. Tsimikas S, Miyanohara A, Hartvigsen K, Merki E, Shaw PX, Chou MY, Pattison J, Torzewski M, Sollors J, Friedmann T, Lai NC, Hammond HK, Getz GS, Reardon CA, Li AC, Banka CL, Witztum JL. Human oxidation-specific antibodies reduce foam cell formation and atherosclerosis progression. *J Am Coll Cardiol*. 2011;58:1715-1727.

30. Rayner KJ, Suarez Y, Davalos A, Parathath S, Fitzgerald ML, Tamehiro N, Fisher EA, Moore KJ, Fernandez-Hernando C. MiR-33 contributes to the regulation of cholesterol homeostasis. *Science*. 2010;328:1570-1573.

31. O'Donnell KA, Wentzel EA, Zeller KI, Dang CV, Mendell JT. c-Myc-regulated microRNAs modulate E2F1 expression. *Nature*. 2005;435:839-843.

32. Zhou R, Hu G, Gong AY, Chen XM. Binding of NF-kappaB p65 subunit to the promoter elements is involved in LPS-induced transactivation of miRNA genes in human biliary epithelial cells. *Nucleic Acids Res*. 2010;38:3222-3232.

33. Li LC, Varghese Z, Moorhead JF, Lee CT, Chen JB, Ruan XZ. Cross-talk between TLR4-MyD88-NF-kappaB and SCAP-SREBP2 pathways mediates macrophage foam cell formation.

Am J Physiol Heart Circ Physiol. 2013;304:H874-884.

34. Grivennikov SI, Karin M. Dangerous liaisons: STAT3 and NF-kappaB collaboration and crosstalk in cancer. *Cytokine Growth Factor Rev*. 2010;21:11-19.

35. Dang CV. MYC, metabolism, cell growth, and tumorigenesis. *Cold Spring Harb Perspect Med*. 2013;3.

36. Chen Z, Shentu TP, Wen L, Johnson DA, Shyy JY. Regulation of SIRT1 by oxidative stress-responsive miRNAs and a systematic approach to identify its role in the endothelium. *Antioxid Redox Signal*. 2013;19:1522-1538.

37. Forstermann U, Sessa WC. Nitric oxide synthases: regulation and function. *Eur Heart J*. 2012;33:829-837, 837a-837d.

38. Kumar A, Hoffman TA, Dericco J, Naqvi A, Jain MK, Irani K. Transcriptional repression of Kruppel like factor-2 by the adaptor protein p66shc. *FASEB J*. 2009;23:4344-4352.

39. Yeung F, Hoberg JE, Ramsey CS, Keller MD, Jones DR, Frye RA, Mayo MW. Modulation of NF-kappaB-dependent transcription and cell survival by the SIRT1 deacetylase. *EMBO J*. 2004;23:2369-2380.

40. Walker AK, Yang F, Jiang K, Ji JY, Watts JL, Purushotham A, Boss O, Hirsch ML, Ribich S, Smith JJ, Israelian K, Westphal CH, Rodgers JT, Shioda T, Elson SL, Mulligan P, Najafi-Shoushtari H, Black JC, Thakur JK, Kadyk LC, Whetstine JR, Mostoslavsky R, Puigserver P, Li X, Dyson NJ, Hart AC, Naar AM. Conserved role of SIRT1 orthologs in fasting-dependent inhibition of the lipid/cholesterol regulator SREBP. *Genes Dev*. 2010;24:1403-1417.

41. Chalkiadaki A; Guarente L. High-fat diet triggers inflammation-induced cleavage of SIRT1 in adipose tissue to promote metabolic dysfunction. *Cell Metab*. 2012;16:180-188.

42. Rautou PE, Leroyer AS, Ramkhelawon B, Devue C, Duflaut D, Vion AC, Nalbone G, Castier Y, Leseche G, Lehoux S, Tedgui A; Boulanger CM. Microparticles from human atherosclerotic plaques promote endothelial ICAM-1-dependent monocyte adhesion and transendothelial migration. *Circ Res*. 2011;108:335-343.

43. de Winther MP, Lutgens E. MiR-92a: at the heart of lipid-driven endothelial dysfunction. *Circ Res*. 2014;114:399-401.

DOI: 10.1161/CIRCULATIONAHA.114.013675

Figure Legends:

Figure 1. H_2O_2, Ang II, and ox-LDL induce SREBP2 and miR-92a in ECs. (A, B) HUVECs were treated with H_2O_2 (100 μM), Ang II (100 nM), or ox-LDL (100 μg/ml) for 16-hour. (A) Cellular proteins were collected for immunoblotting (IB) of SREBP2 precursor and mature form of SREBP2 [SREBP2(N)]. Bar graphs are densitometry quantifications of the ratios of SREBP2 precursor or mature SREBP2 to β-actin level. (B) RNA were collected for RT-qPCR analysis of mRNA encoding LDLR and squalene synthase. (C-E) Taqman miRNA qPCR analysis of miR-92a level in HUVECs treated with various concentrations of H_2O_2, Ang II, and ox-LDL for 16-hour. (F-H) HUVECs were pretreated with EUK-134 (1 μM) for 2-hour and then incubated with H_2O_2, Ang II or ox-LDL for 16-hour. SREBP2 was detected by IB and miR-92a level by Taqman miRNA qPCR. Data are mean±SD from at least 3 independent experiments. * $p < 0.05$ compared to respective control or between indicated groups.

Figure 2. SREBP2 transactivates miR-92a under oxidative stress. (A) Bioinformatics analysis of SREs in the promoter region of human miR-17-92 cluster. (B) RT-qPCR and Taqman miRNA qPCR analyses of SREBP2 and miR-92a levels in HUVECs infected with Ad-null or Ad-SREBP2(N). (C) miR-92a level in HUVECs transfected with SREBP2 siRNA (10 nM) or control RNA and then treated with H_2O_2. (D,E) ChIP assays were performed with SREBP2 antibody or a nonspecific IgG in extracts from HUVECs treated with H_2O_2 (in D) or infected with Ad-SREBP2(N) (in E). The enrichment of SREBP2(N) binding to the putative SREs in the promoter region of miR-17-92 was quantified by qPCR, with non-treated group (in D) or Ad-null group (in E) set to 1. * $p < 0.05$ compared to respective control or between indicated groups.

Figure 3. Oxidative stress-induced miR-92a increases endothelial innate immunity. IB of caspase-1 and IL-1β in HUVECs (A) treated with H_2O_2 (100 μM), Ang II (100 nM) or ox-LDL (100 μg/ml) for 16-hour; (C) transfected with control RNA or pre-miR-92a (20 nM) for 72-hour; or (E) transfected with control RNA or anti-miR-92a for 48-hour before H_2O_2 treatment for 24-hour. Quantification in (B,D,F) is relative expression of caspase-1 and IL-1β, to that of β-actin. (G,H) Flow cytometry quantification of active caspase-1 in HUVECs transfected as in (E). Histograms in (G) are representative results and data in (H) are mean±SD from 5 independent experiments, with the percentage of caspase-1^+ cell in control RNA group set to 1.

Figure 4. Oxidative stress-induced miR-92a targets SIRT1, KLF2, and KLF4 to increase endothelial innate immunity. (A-C) Following 16-hour treatment of H_2O_2, Ang II, or ox-LDL, AGO-miRISC was immunoprecipitated and the AGO-bound miR-92a and SIRT1, KLF2 and KLF4 mRNAs were quantified by RT-qPCR. Mouse IgG was used as an isotype control. (D-F) BAECs were transfected with luciferase reporter containing 5 tandem miR-92a binding/responsive elements (MREs) in SIRT1 3'UTR, 2 tandem MREs in KLF2 3'-UTR, or KLF4 3'-UTR together with anti-miR-92a or control RNA for 24-hour and then treated with H_2O_2, Ang II, or ox-LDL for 16-hour. Luciferase activity was measured and normalized to that of Renilla. (G-I) HUVECs were transfected with anti-miR-92a or control RNA for 48-hour before H_2O_2 treatment. (J) HUVECs were infected with Ad-null or Ad-SREBP2(N) before transfection with control RNA or anti-miR-92a. (K, L) HUVECs were infected with Ad-null or Ad-SIRT1, Ad-KLF2, and Ad-KLF4 together for 48 h, and then treated with H_2O_2 for 24-hour. The mRNA levels of SIRT1, KLF2 and KLF4 were assessed by RT-qPCR (G). The levels of proteins shown in (H, J, K) were revealed by IB. (I, L) The NO level in the medium was

measured by a fluorometric assay (I, L).

Figure 5. Oxidative stress induction of miR-92a and inflammasome *in vivo*. (A,B) Taqman miRNA qPCR of miR-92a level in whole aortas isolated from 8-week-old C57BL6 with or without Ang II infusion (A) and C57BL6 at 3 month- and 12 month-old (B). (C,D) *hsp70:*IK17-EGFP Tg zebrafish were fed a normal diet or HCD. IK17-EGFP was heat shock-induced (HS) in one group of HCD-fed fish. The trunk regions were collected for miR-92a qPCR (C). IK17 induction was confirmed by visualization of EGFP (D). Bar = 0.1 cm. (E,F) RT-qPCR analysis of miR-92a and mRNA levels of various genes in intima isolated from EC-SREBP2(N)-Tg and that from wild-type littermates (WT) pooled from 4 animals in each group (E) and carotid arteries of EC-SREBP2(N)-Tg with local delivery of control LNA (LNA-Ctrl) or LNA-92a (F). (G) Vasodilatory function of carotid arteries from EC-SREBP2(N) Tg mice treated as in (F). n denotes number of animals used and * indicates $p < 0.05$ compared to respective control or between indicated groups.

Figure 6. Inhibition of miR-92a mitigates oxidative stress-induced atherosclerosis in mice. (A, B) *En face* imaging of mouse aorta and quantification of lesion area in $ApoE^{-/-}$/EC-SREBP2(N) mice fed normal chow and infused with Ang II (1 μg/min/kg) for 28-day. The age of mice and tail-vein injection of LNA are as indicated. Bar = 0.5 cm. (C) Caspase-1 in lung ECs isolated from 3-month-old $ApoE^{-/-}$/EC-SREBP2(N) mice receiving LNA-Ctrl or LNA-92a was detected by IB. (D) miR-92a was detected in $CD31^{+}$ microparticles (MPs) isolated from sera of 3-month-old $ApoE^{-/-}$ or $ApoE^{-/-}$/EC-SREBP2(N) mice treated with Ang II. IgG was used as an isotype control in MP isolation from sera of $ApoE^{-/-}$/EC-SREBP2(N) mice.

DOI: 10.1161/CIRCULATIONAHA.114.013675

Figure 7. miR-92a inversely correlates with EC function in human patients. (A-C) Correlations between circulating miR-92a level and (A) FMD; (B) serum IL-1β concentration; and (C) miR-92a level in serum $CD31^+$ MPs from patients with stable CAD. While n denotes number of patients, r_s is Spearman's correlation coefficient. (D) Schematic illustration of the hypothesis "oxidative stress activates EC innate immune response and impairs EC function through induction of SREBP2-miR-92a". SREBP2 transactivation of miR-92a, through targeting SIRT1, KLF2, and KLF4, activates inflammasome and inhibits eNOS-derived NO bioavailability. Therefore, SREBP2-miR-92a-inflammasome may be a crucial pathway linking oxidative stress, inflammation, and endothelial dysfunction.

Figure 1

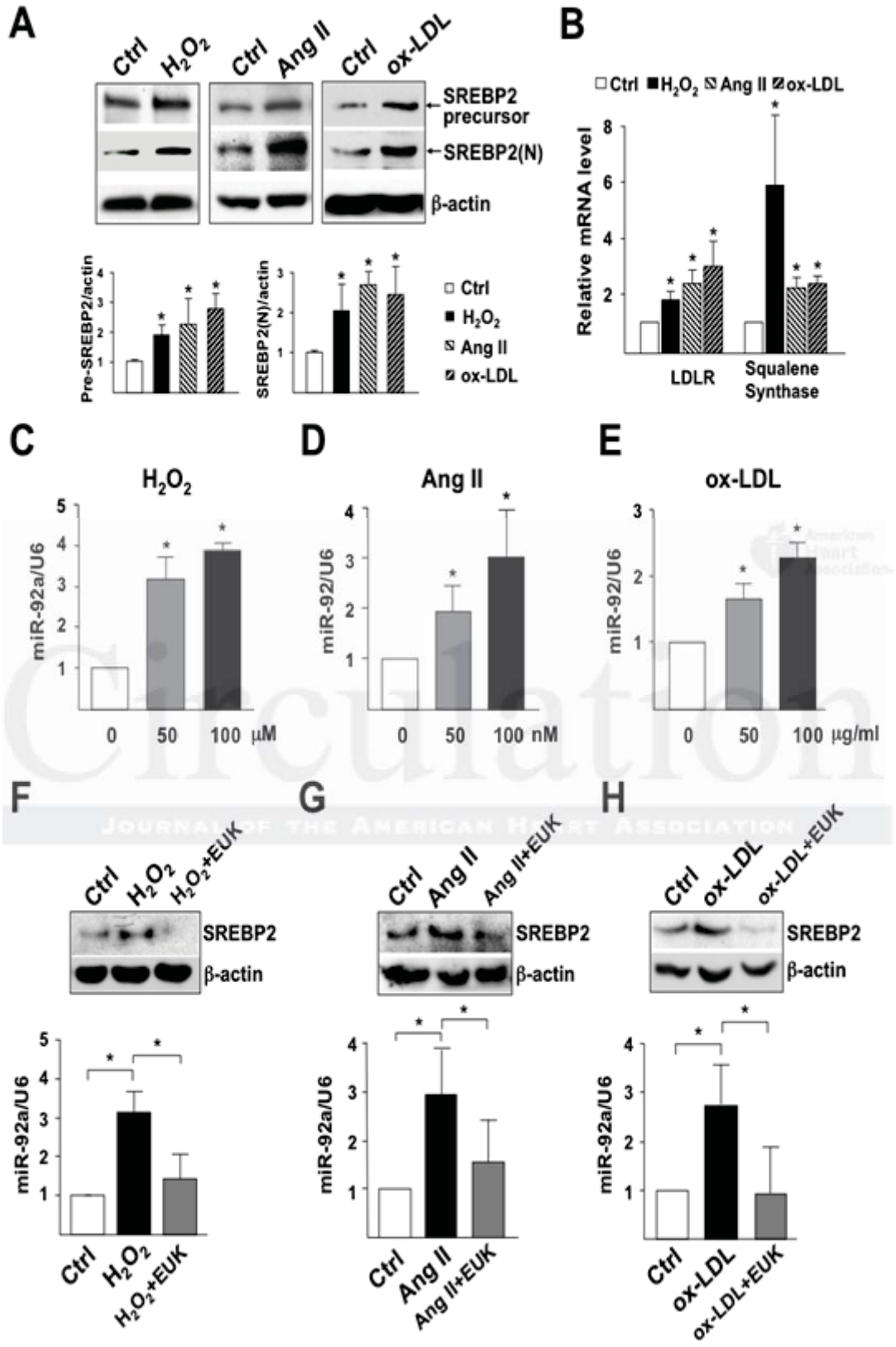

Figure 2

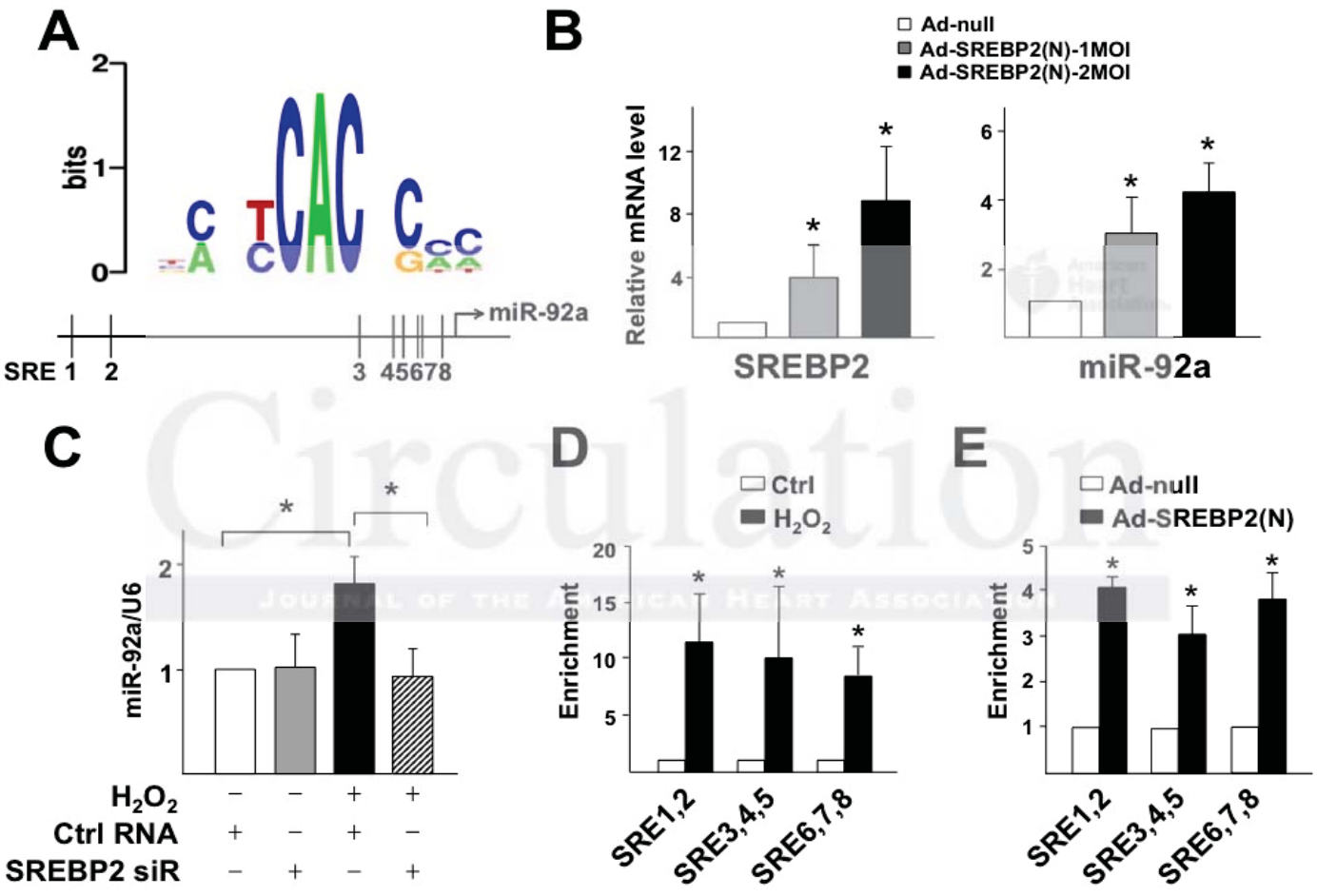

Figure 3

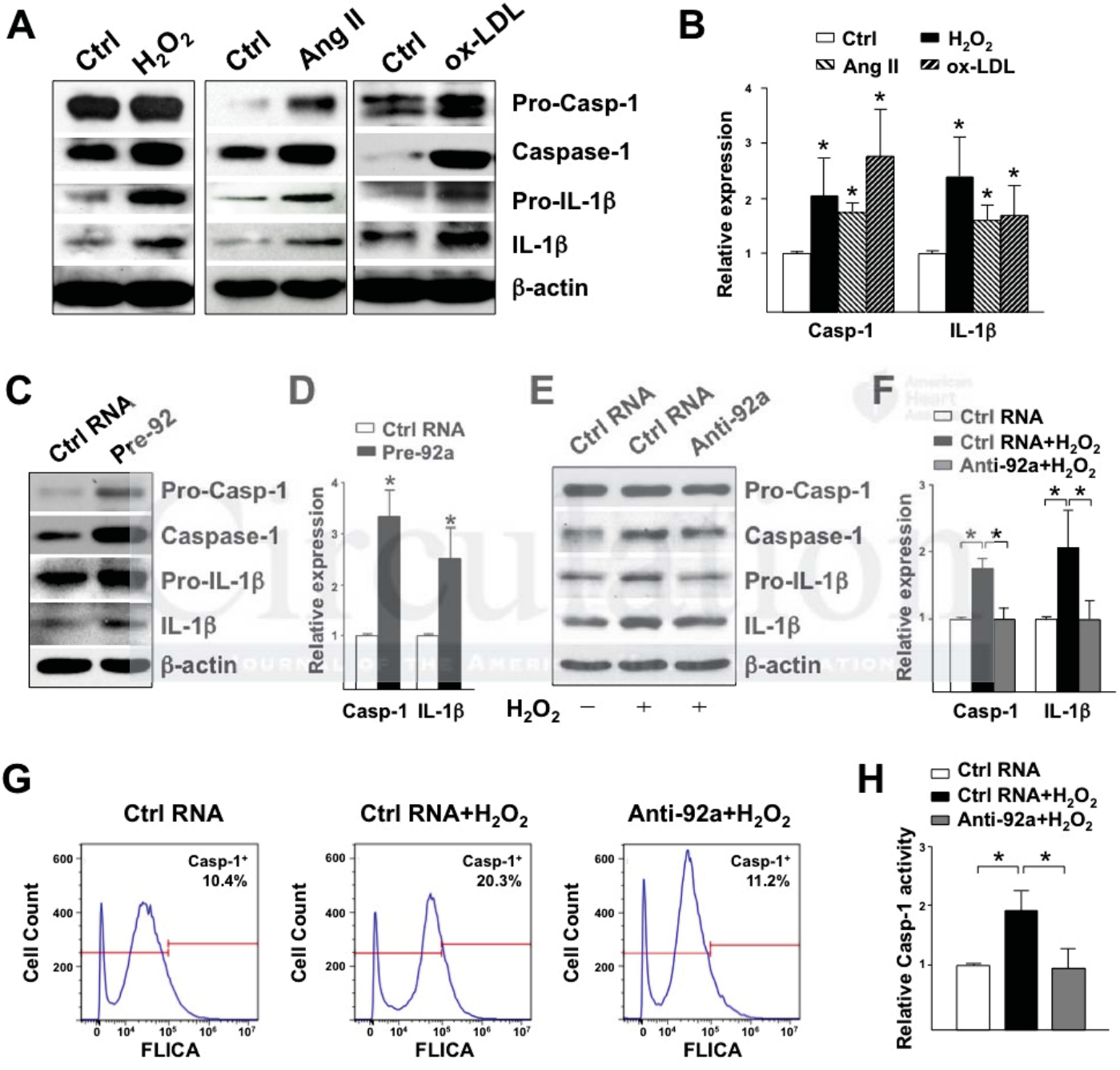

Figure 4

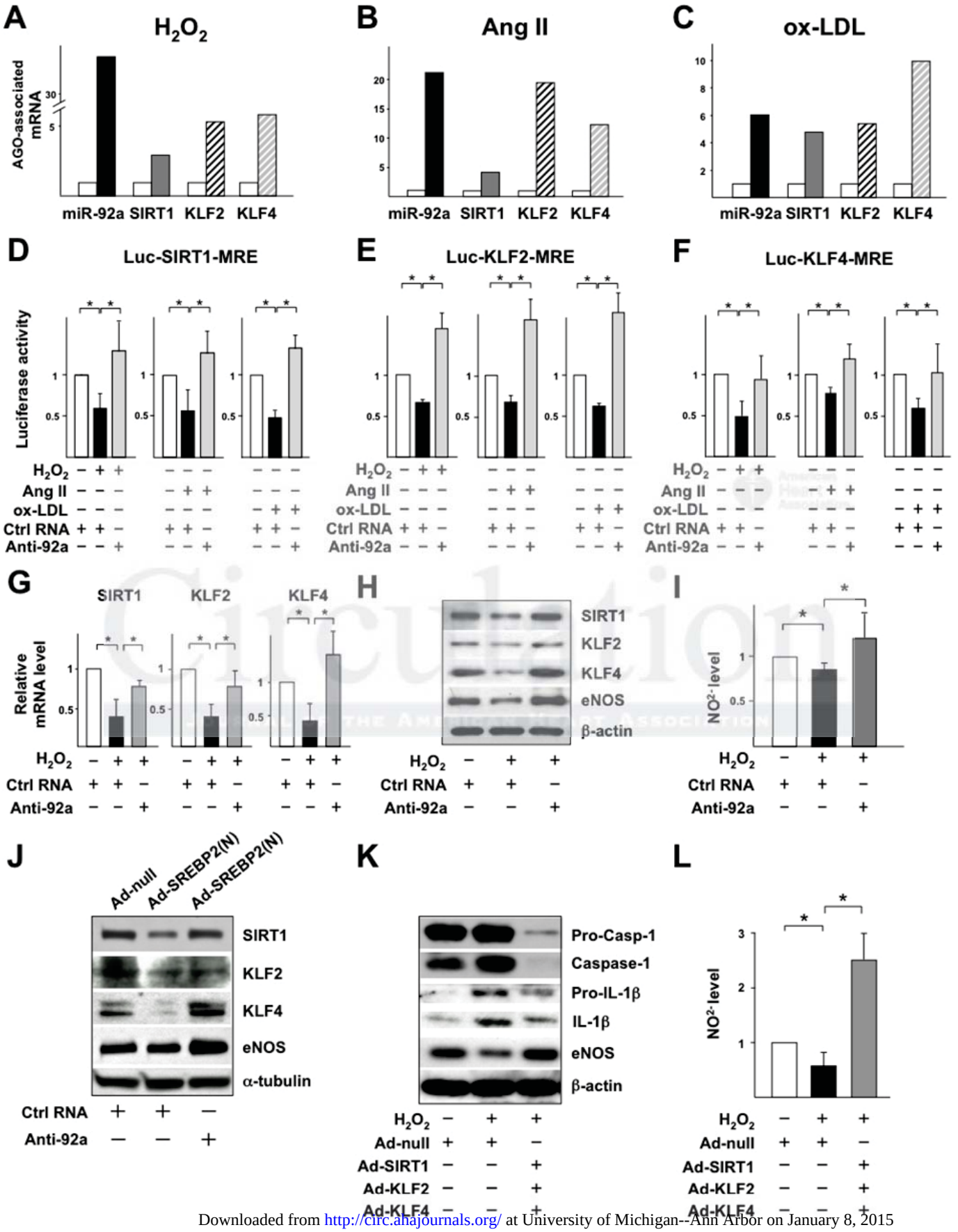

Figure 5

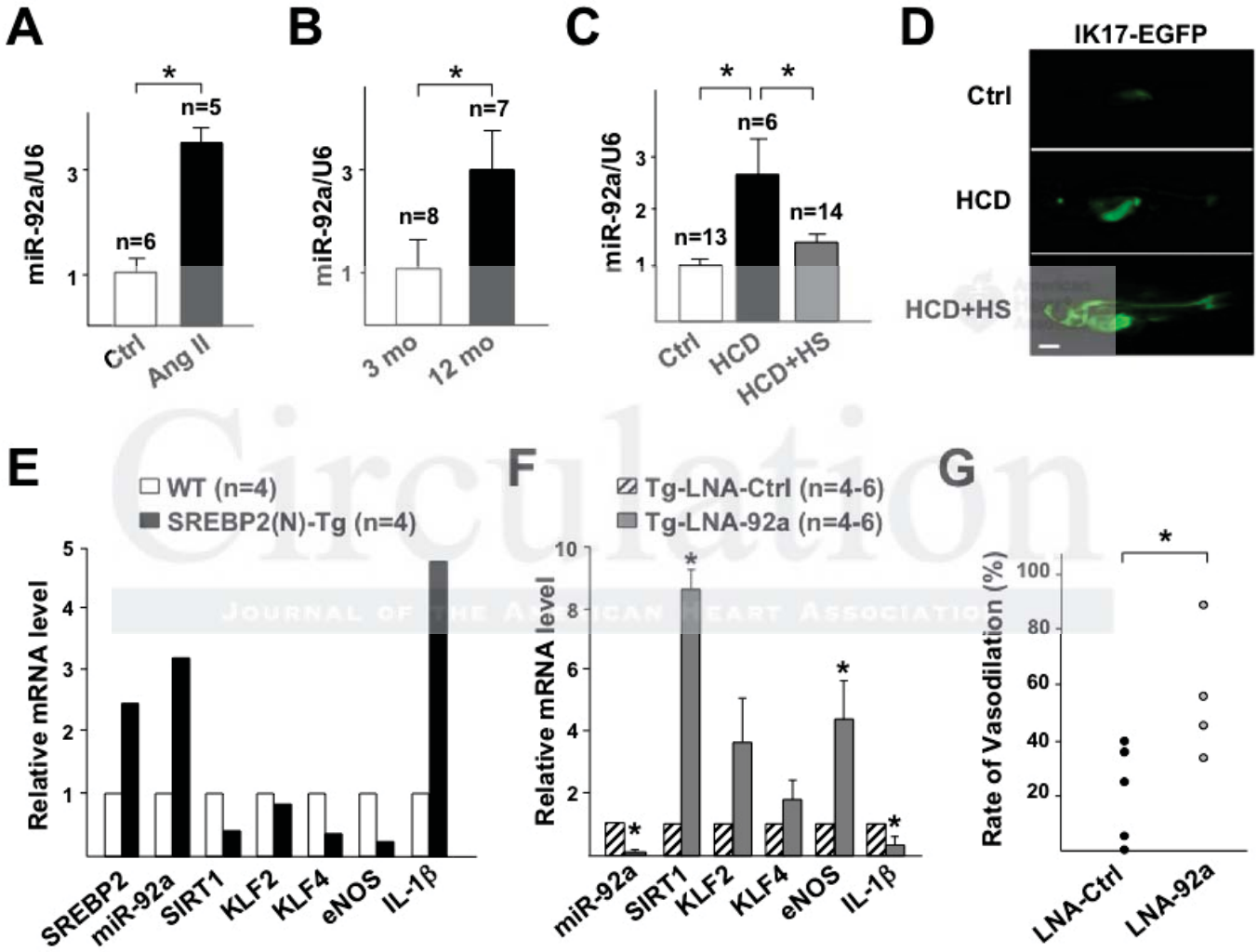

Figure 6

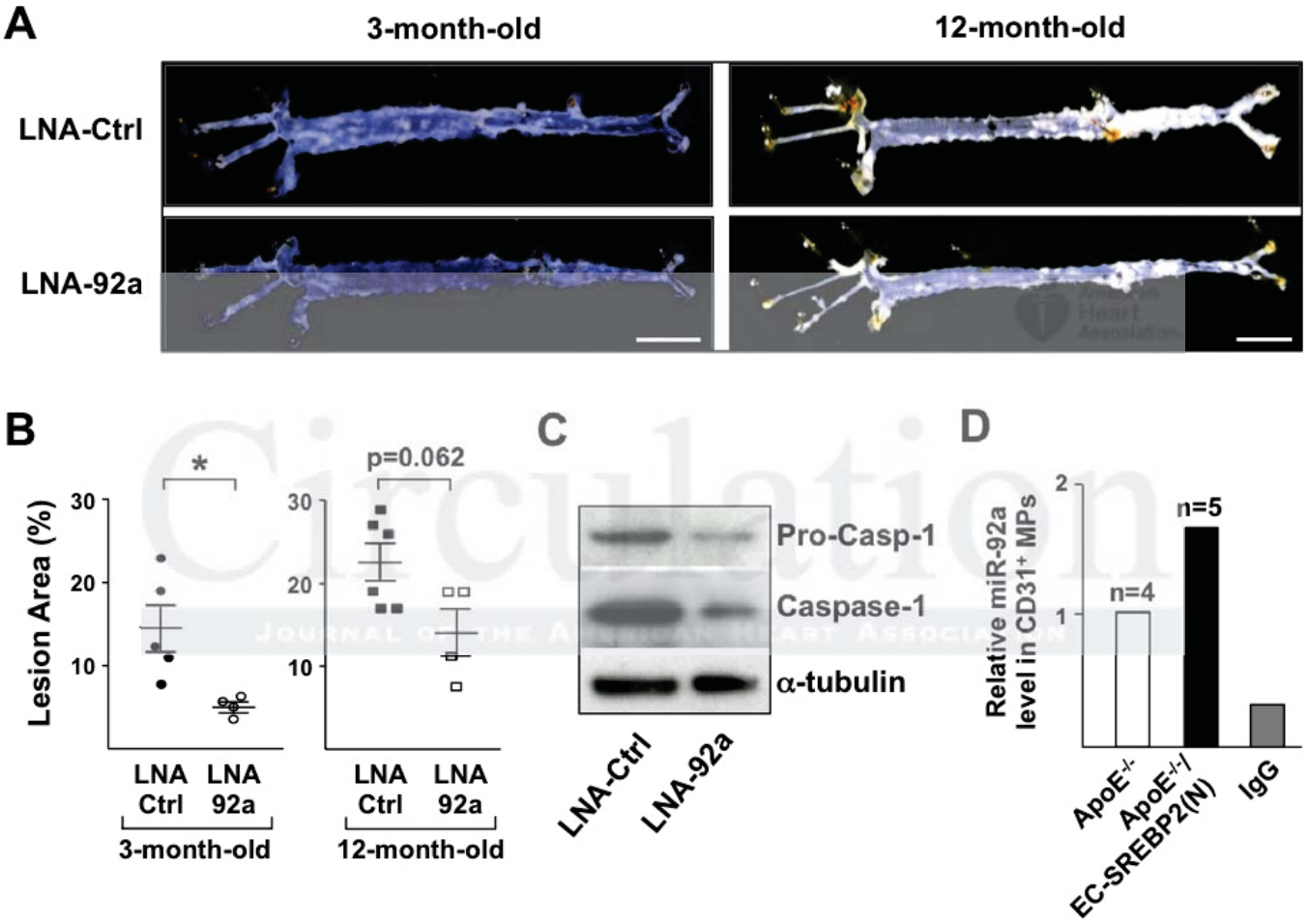

Figure 7

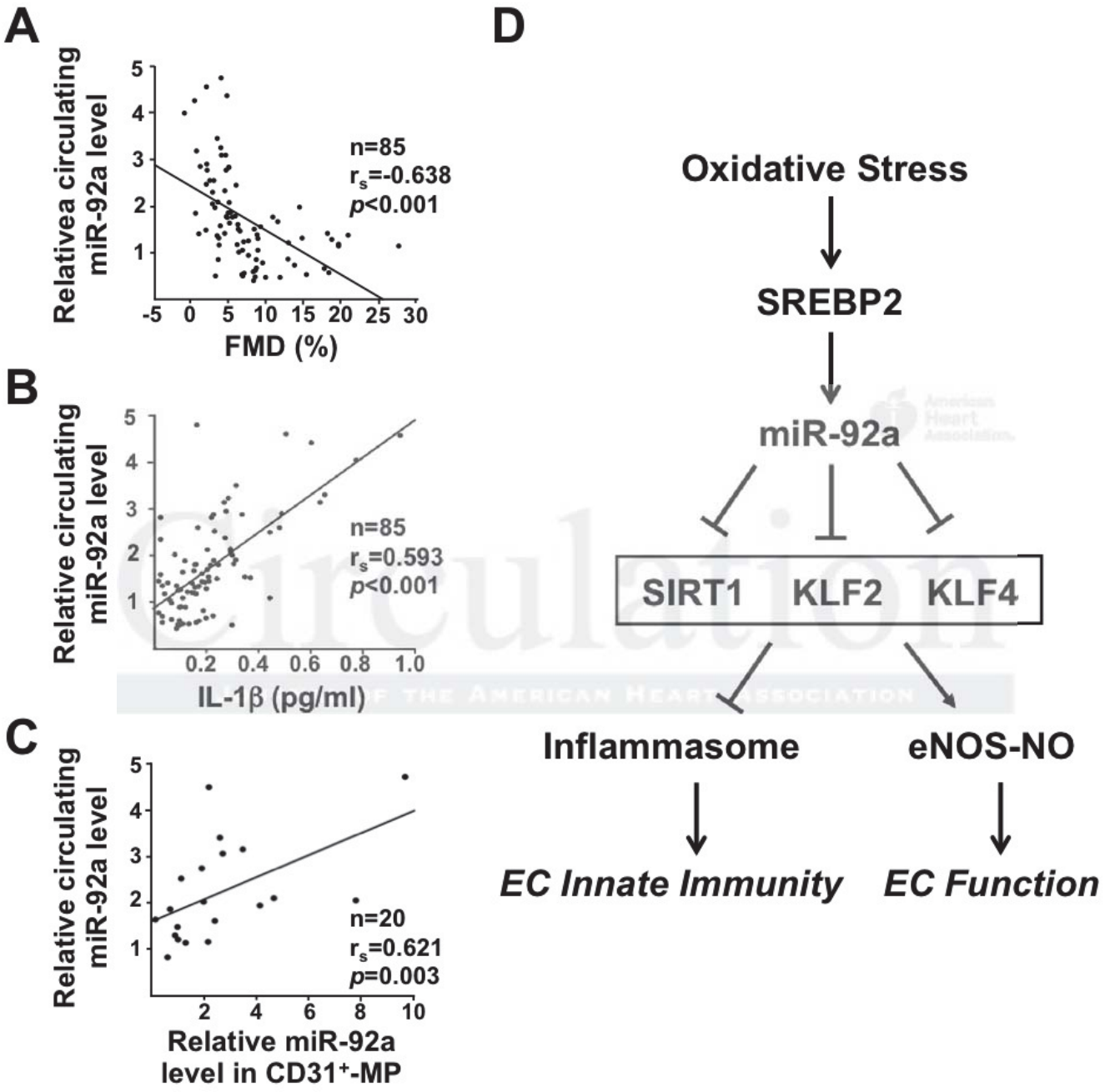

SUPPLEMENTAL MATERIAL

Supplemental Methods

RT-qPCR analysis of mRNA and miRNA

RNA from cultured cells or tissues was extracted by use of TRIzol (Invitrogen) and RNA from sera was isolated with a TRIzol LS protocol (Invitrogen). For mRNA quantification, total RNA was reverse-transcribed (RT) by use of the iScript cDNA synthesis kit (Biorad), followed by quantitative real-time PCR (qPCR) with SYBR Green (Bio-Red) and a Bio-Red CFX-96 real-time system. The relative level of mRNA was calculated by the ΔΔCq method with β-actin as an internal control. For miRNA quantification, TaqMan miRNA assay was performed following manufacturer's protocol (Life Technologies). U6 was detected as the internal control in cultured cells and tissues from animals. To quantify miR-92 level in sera or MPs, a *C. elegans* miRNA, i.e. Cel-miR-39 was spiked in at 2 nM before RNA extraction, which level was used as the internal control.

Transcription factor and miRNA binding sites prediction

The potential SREBP2 binding sites in miR-17-92 promoter regions were predicted by use of TRANSFAC[1] and MATCH[2]. The promoter regions were defined as -3000 ~ +1000 bp from the transcriptional start site (TSS) of the miR-17-92 cluster. The putative binding sites were designated SRE1-SRE8. To predict miR-92a targeting SIRT1 3'UTR, we used miRanda[3] to scan cross-species conserved 3'UTRs of SIRT1 mRNA.

Sequences of primers used in mRNA RT-qPCR and ChIP

Gene-specific primer sequences for RT-qPCR:

Gene	Species	Sequence	
SIRT1	Human	Forward	AAGTTGACTGTGAAGCTGTACG
		Reverse	TGCTACTGGTCTTACTTTGAGGG
SIRT1	Mouse	Forward	TGATTGGCACCGATCCTCG
		Reverse	CCACAGCGTCATATCATCCAG
KLF2	Human	Forward	TTCGGTCTCTTCGACGACG
		Reverse	TGCGAACTCTTGGTGTAGGTC
KLF2	Mouse	Forward	GAGCCTATCTTGCCGTCCTTT
		Reverse	CAGGTTGTTTAGGTCCTCATC
KLF4	Human	Forward	CCCACATGAAGCGACTTCCC
		Reverse	CAGGTCCAGGAGATCGTTGAA
KLF4	Mouse	Forward	AGGAACTCTCTCACATGAAGCG
		Reverse	GGTCGTTGAACTCCTCGGTC
β-actin	Human	Forward	CATGTACGTTGCTATCCAGGC
		Reverse	CTCCTTAATGTCACGCACGAT
β-actin	Mouse	Forward	GGCTGTATTCCCCTCCATCG
		Reverse	CCAGTTGGTAACAATGCCATGT
eNOS	Human	Forward	TGGCTTTCCCTTCCAGTTC
		Reverse	AGAGGCGTTTTGCTCCTTC
eNOS	Mouse	Forward	CACCTACGACACCCTCAGTG
		Reverse	CTTGACCCAATAGCTGCTCAG
SREBP2	Human	Forward	CCCTGGGAGACATCGACGA
		Reverse	CGTTGCACTGAAGGGTCCA
SREBP2	Mouse	Forward	GCAGCAACGGGACCATTCT
		Reverse	CCCCATGACTAAGTCCTTCAACT
Squalene synthase	Human	Forward	CTGGTGCGCTTCCGGATCGG
		Reverse	ACTGCGTTGCGCATTTCCCC
LDLR	Human	Forward	TCACCAAGCTCTGGGCGACG
		Reverse	GTAGCCGTCCTGGTTGTGGCA
IL-1β	Mouse	Forward	ATGAGAGCATCCAGCTTCAA
		Reverse	TGAAGGAAAAGAAGGTGCTC

Caspase-1	Mouse	Forward	AGGCATGCCGTGGAGAGAAACAA
		Reverse	AGCCCCTGACAGGATGTCTCCA
α-tubulin	Human	Forward	GCTGGGAACTGTACTGCCTG
		Reverse	AGGTCCACAAACACTGCTCTG
5s rRNA	Human	Forward	TACGGCCATACCACCCTGAA
		Reverse	GCGGTCTCCCATCCAAGTAC

For ChIP assay, the following primer sets were designed on the basis of the putative SREs in the miR-17-92 promoter region:

SRE	Location	Primer Sequence	
1, 2	-1731, -1556	Forward	TGCGTCTTCCAAAATCCTGATTAC
		Reverse	AATTAGAATGGTTGAGGCGGGG
3, 4, 5	-402, -244, -186	Forward	TTAACGGAGGGCGTGCCG
		Reverse	TAAATACGGACAAGCCCCACTC
6, 7, 8	-135, -129, -52	Forward	ATTTACGTTGAGGCGGGAGC
		Reverse	GCCTGCGCTTTACTACGACC

Antibodies and immunoblotting (IB)

Antibodies against SIRT1, KLF4, eNOS, acetyl-p53 (K382), acetyl-NF-κB (K310), caspase-1, β-actin, and horseradish peroxidase conjugated with anti-rabbit or anti-mouse IgG were from Cell Signaling. Anti-IL-1β was from Abcam and anti-SREBP2 was from BD Biosciences Pharmingen. The custom-made anti-KLF2 from Genetex was previously described.[4] Protein extracts from cultured cells or tissues were resolved by SDS-PAGE and transferred to PVDF membrane. IB was performed with respective antibodies.

Transfection and infection

Control RNA, respective plasmids, siRNAs, pre-miR-92, or anti-miR-92 were transfected into ECs or HEK-293 cells by use of Lipofectamine 2000 RNAi Max (Invitrogen) in various experiments with subsequent treatment with H_2O_2, Ang II, or ox-LDL. SREBP2(N), KLF2, KLF4 or SIRT1 were overexpressed by adenovirus (Ad)-driven ectopic expression in HUVECs at 50% confluence with. Control cells were infected by Ad-null expression at the same MOI.

Luciferase reporter plasmids and luciferase assay

To generate the pMIR-Luc-SIRT1-3'UTR reporter [Luc-SIRT1(WT)], the full-length human SIRT1 3'UTR was subcloned into the pMIR-REPORT vector (Ambion). With this construct, Luc-SIRT1(MUT) was created by introducing a CA→GT mutation into the most conserved miR-92a target site in SIRT1 3'UTR, particularly in the region complementary to miR-92a seed sequence (Supplemental Figure 2A). To create the reporter containing the specific miR-92a target sites in SIRT1 3'UTR, (i.e. Luc-SIRT1-MRE), 4 tandem copies of the most conserved miR-92a binding sequences were subcloned downstream of luciferase into pMIR-REPORT. Luc-KLF2-MRE and Luc-KLF4-MRE were previously described.[4,5] Luciferase reporter constructs were co-transfected with renilla luciferase as a transfection control with or without pre-miR/anti-miR or control RNA. Luciferase activity was measured by use of the Dual-Glo Luciferase Reporter Assay Kit (Promega).

***Ex vivo* assessment of flow-mediated vasodilation**

We used 8- to 10-week-old male mice to evaluate the flow-mediated vasodilation as described.[4] To compare the vasoreactivity of EC-SREBP2(N)-Tg mice and their wild-type littermates, right carotid arteries were dissected and cannulated with the perfusion chamber connected to the SoftEdge Acquisition Subsystem (Living Systems, Burlington, VT). The vessels were perfused with 37°C solution containing 130 mM NaCl, 10 mM HEPES, 6 mM

glucose, 4 mM KCl, 4 mM $NaHCO_3$, 1.8 mM $CaCl_2$, 1.18 mM KH_2PO_4, 1.2 mM $MgSO_4$ and 0.025 mM EDTA, pH 7.4. Phenylephrine was added at 1-3 μM to the solution to obtain maximal constriction. Subsequently, flow at 400 μl/min was applied to the vessels and the external diameter of the vessels was monitored. In another experiment, to evaluate the effect of LNA, right carotid arteries from EC-SREBP2(N)-Tg mice were dissected and then coated with 30% F-127 pluronic gel (Sigma) mixed with 30 μg of LNA-92a or control LNA. Five days post-surgery, mice were sacrificed and the pluronic gel-coated vessels were isolated for procedures described above.

Isolation of lung ECs, MPs, and quantification of atherosclerotic lesions

Lung ECs were isolated as previously described[6] with modification. Briefly, dissected lungs underwent treatment with Type I collagenase and further sorting with CD31 (PECAM-1) and CD102 (ICAM-2) antibodies (BD Biosciences). Procedures isolating $CD31^+$ MPs were adapted from Amabile *et al.*[7] and included 20,000g centrifugation for 45 min and IP with anti-CD31. IgG was used as an isotype control of IP. Mouse aortas were isolated and lesion area was measured by use of Image Pro Plus 6.0 (Media Cybernetics) and expressed as a percentage of the total area of aorta.

Assessment of FMD in patients

Briefly, all subjects were asked to fast and withhold all medications for 24 h before the measurement of FMD. To minimize the mental stress, care was taken to maximize patients' comfort, and the procedure was performed in a quiet and air-conditioned room (25°C). The left arm was stabilized with a cushion, and a sphygmomanometric cuff was placed on the forearm. A baseline image was acquired, and blood flow was estimated by time-averaging the pulsed

Doppler velocity signals obtained from a mid-artery sample volume. The cuff was then inflated to at least 50 mm Hg above systolic pressure to occlude arteries for 5 minutes and released abruptly. A mid-artery pulsed Doppler signal was obtained immediately upon cuff release and no later than 15 sec after cuff deflation to assess hyperemic velocity. Post-occlusion diameters were obtained at 60, 80, 100 and 120 sec after deflation. EC-dependent FMD was calculated as the maximal post-occlusion diameter relative to the average pre-occlusion diameters.

Supplemental Table 1 Baseline Characteristics of CAD Patients

	All Subjects (n = 85)
Age (years)	68.4 ± 11.4
Male	58 (68%)
Diabetes	33 (39%)
Hypertension	66 (78%)
BMI	25.6 ± 3.6
Current smoker	10 (12%)
Lipid profile	
Total cholesterol (mg/dL)	155.6 ± 28.6
Triglycerides (mg/dL)	121.9 ± 65.8
HDL (mg/dL)	40.7 ± 11.4
LDL (mg/dL)	88.4 ± 25.5
Fasting glucose (mg/dL)	111.4 ± 33.1
HbA1c (%)	6.5 ± 1.3
BUN (mg/dL)	20.3 ± 12.2
Serum creatinine (mg/dL)	1.6 ± 2.0
Uric acid (mg/dL)	6.2 ± 2.0
Systolic BP (mmHg)	133.0 ± 18.9
Diastolic BP (mmHg)	76.8 ± 10.5
LVEF (%)	54.1 ± 16.9
Medications	
ACE-I/ARB	39 (46%)
Calcium channel blockers	28 (33%)
Beta-blockers	29 (34%)
Thiazides	11 (13%)
Statin	33 (39%)
Nitrates	27 (32%)

Values are mean ± SD or number (%).

BMI, body mass index; HDL, high-density lipoprotein; LDL, low-density lipoprotein; BUN, blood urine nitrogen; BP, blood pressure; LVEF, left ventricular ejection fraction; ACE-I, angiotensin-converting enzyme inhibitor; ARB, angiotensin II receptor blocker.

Supplemental Table 2 Putative SREs in Human and Mouse miR-17-92 Promoter

SRE	Strand	Distance to TSS	SRE in Human	SRE in Mouse	PhastConsv Score
1	+	-1731	GTAGTCACAGAAAAT	ATAGATACAGAGAAT	0.77
2	-	-1556	TTCATCACACTCTCT	TTCATCA----CTCT	0.61
3	-	-402	CGCGCCACGCCTCCG	CGCGCCACGCCCCCG	0.88
4	-	-244	CCAATCACCGCAGGC	CCAATCACCGCAGGC	0.96
5	-	-186	AGCCCCACTCCCTCA	AGCCCCACTCCCTCA	0.98
6	+	-135	TCATTCACCCACATG	TCATTCACCCACATG	0.99
7	-	-52	GTCCCCACCCCCTCG	GTCCCCACCCC-TCG	0.78
8	+	-129	ACCCACATGGT	ACCCACATGGT	0.98

Putative SREs in human and mouse genomes were predicted by TRANSFAC and MATCH. The conservation scores were calculated by PhastCons in the UCSC Genome Brower. Sequences in red indicate the core SRE sequences in the human miR-17-92 promoter region.

Supplemental Table 3 Putative SREs in Zebrafish miR-92a Promoter

Chromosome	Location	Strand	SRE
Chr 9	55417585	-	GTGATGTGGACA
Chr 9	55418022	-	ATATTGTGGCAA
Chr 9	55420624	+	AGGCCACCATCA
Chr 9	55420758	+	TTGCCAGCCCCT
Chr 9	55422020	-	CGAAAGTGGCGC
Chr 9	55422249	-	TTTAGCTGGCAG
Chr 9	55425168	+	GAGCCACCGTGT
Chr 9	55425230	-	AGGCAGTGGCGC
Chr 9	55425538	-	CCGCTGTGGCGA
Chr 9	55425905	-	TTGCTGTGGCTC
Chr 9	55425936	-	TTGCGGTGGCTC
Chr 9	55426405	+	TCGCCACAGCGG
Chr 1	2799351	+	TTGCCAGCTCAC
Chr 1	2801806	-	GTGAGCTGGCAA
Chr 1	2802241	+	TTGCCACTGTAG
Chr 1	2804493	+	GCGCCACTTTTG
Chr 1	2804632	-	GAGCAGTGGCTG
Chr 1	2804845	-	AGTAAGTGGCGC
Chr 1	2804867	+	TCTCCACCTCCA
Chr 1	2805502	+	GCACCACCGCGC
Chr 1	2805695	+	GCGCCACACAGA
Chr 1	2806456	-	TGATGGTGGCCT
Chr 1	2806824	-	TGATTGTGGCAG
Chr 1	2807363	-	GAGGGGTGGTCT
Chr 1	2808825	+	TTACCACCTGAA

The transcription starting site (TSS) of dre-miR-92a (i.e., zebrafish miR-92a) was predicted based on RNA-seq data from ENSEMBL genome browser. The putative SREs were searched with same methods as for human and mouse genes.

Supplemental Figure 1

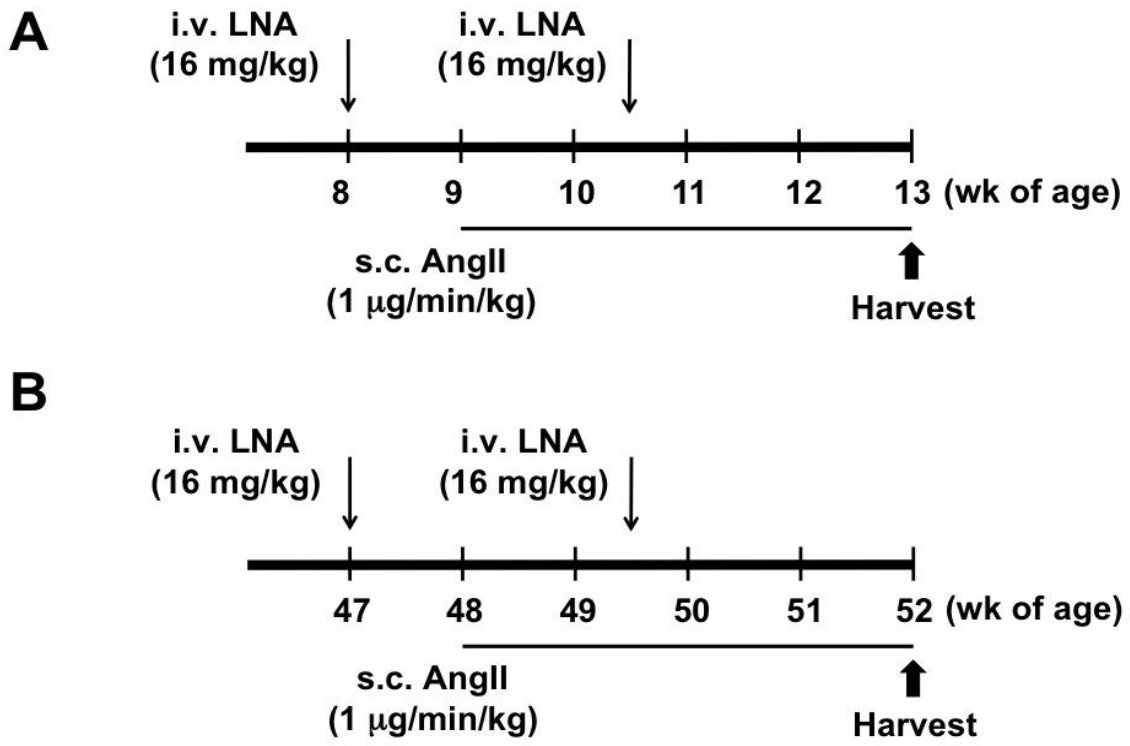

Supplemental Figure 2

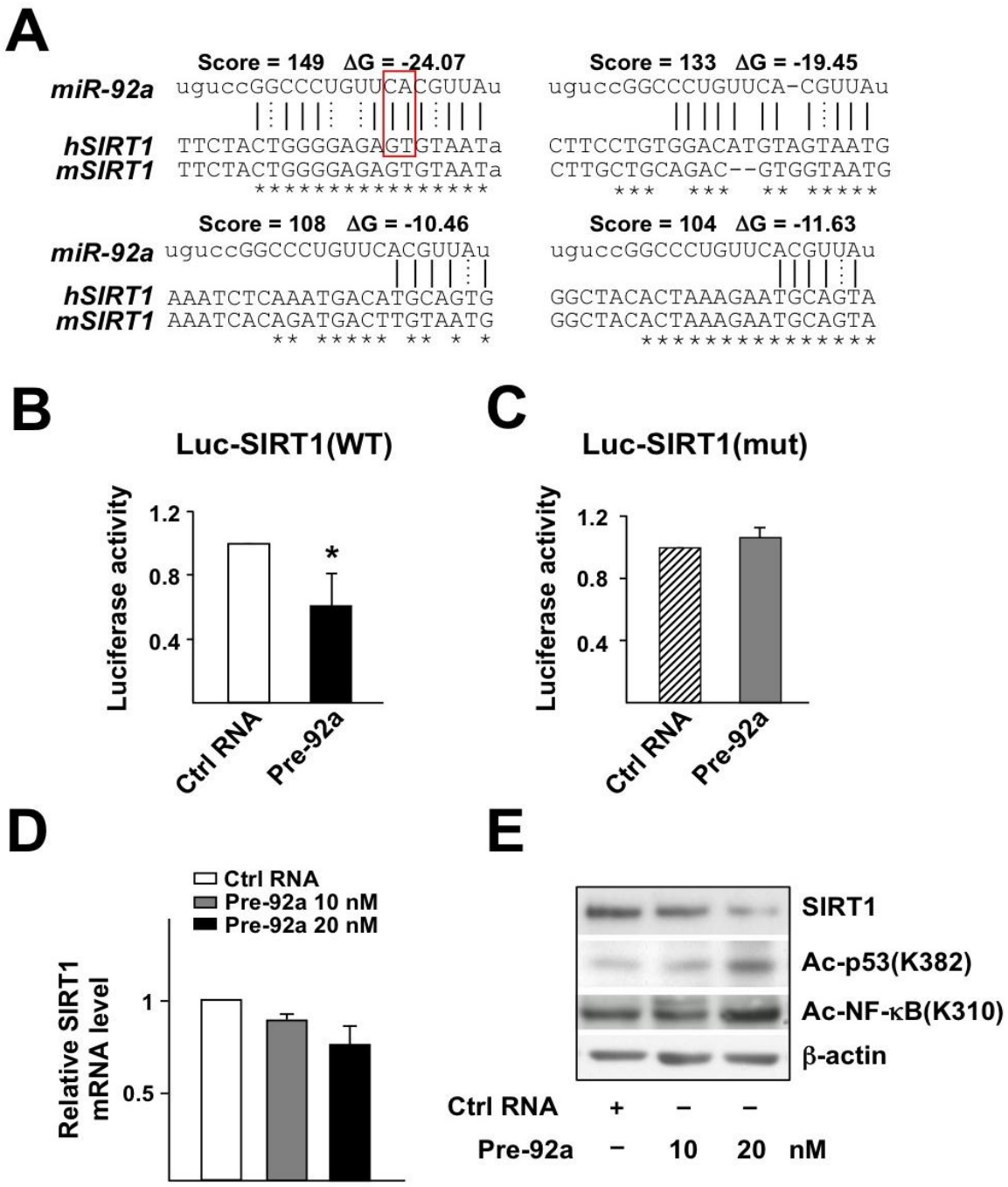

Supplemental Figure 3

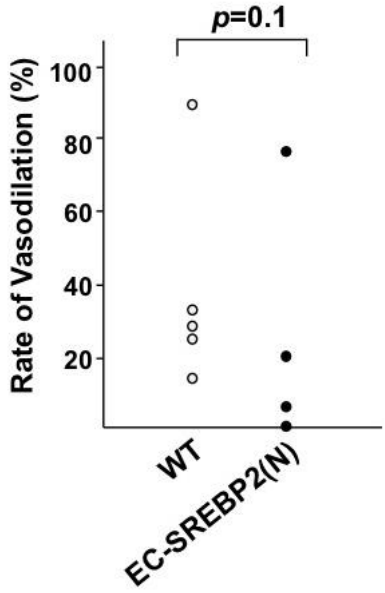

Supplemental Figure 4

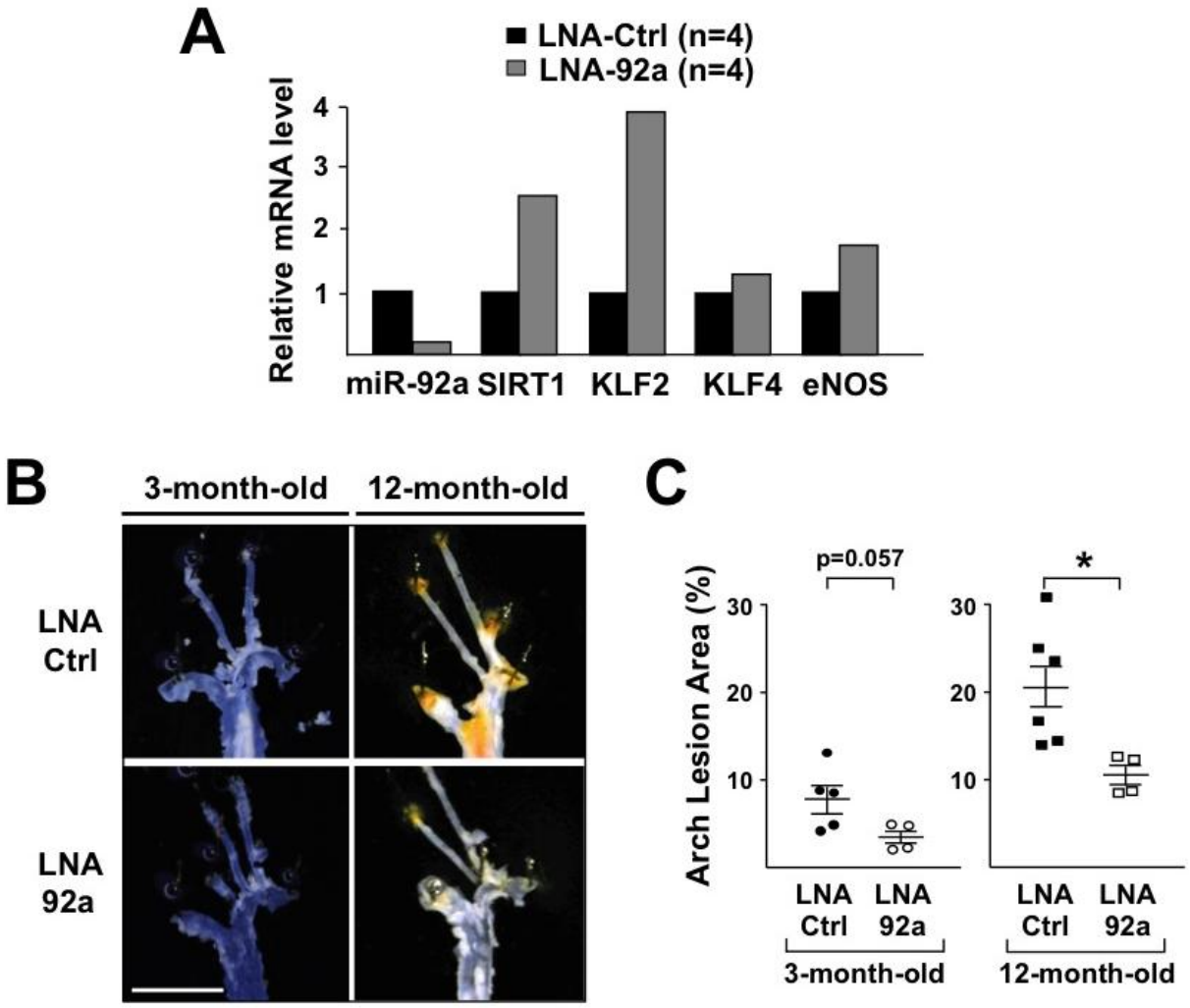

Supplemental Figure 5

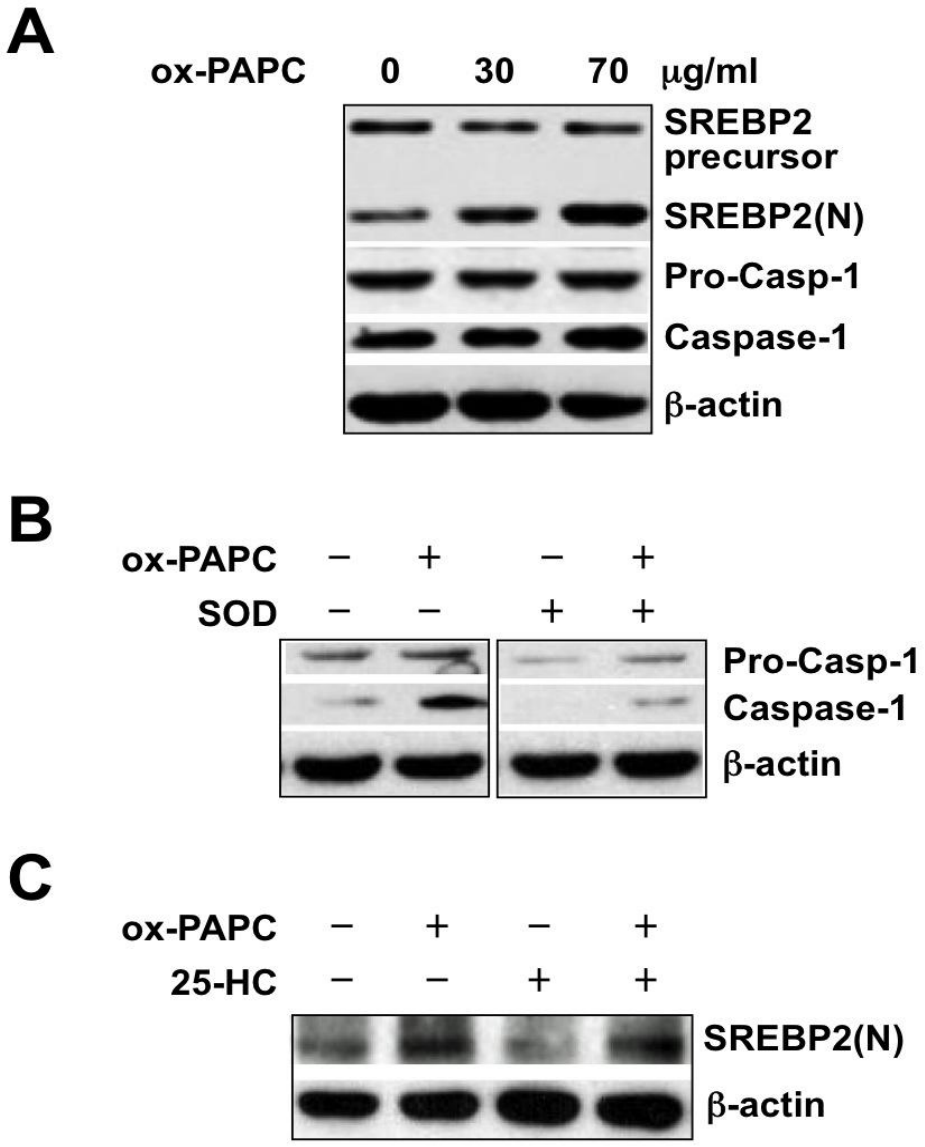

Supplemental Figure 6

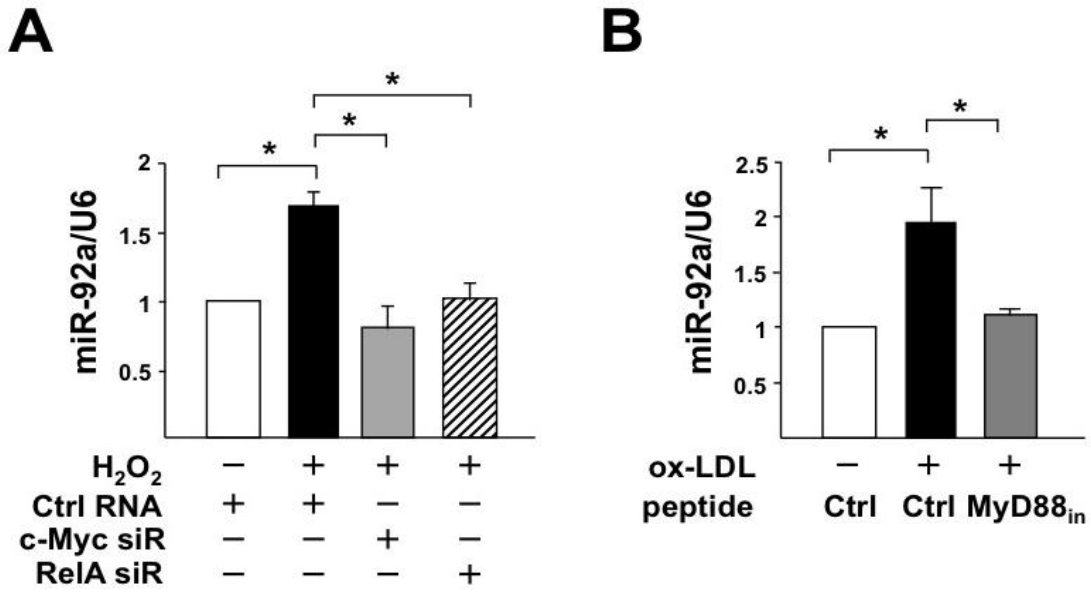

Supplemental Figure 7

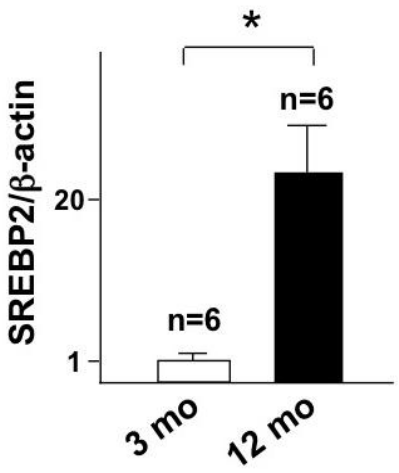

Supplemental Figure Legends

Supplemental Figure 1. Experimental design of mouse study involving LNA injection and Ang II infusion. One week before Ang II infusion, control LNA or LNA-92a were *i.v.* injected at 16 mg/kg BW through tail-vein. Osmotic minipumps filled with Ang II solution were implanted subcutaneously into the dorsal side of mice. Ang II was released at 1 μg/kg/min for 4-week. The second dose of LNA was given 10 days (~1.5 week) after the minipump implantation. The animals were sacrificed at the end of 4-week post minipump implantation.

Supplemental Figure 2. miR-92a targets SIRT1 3'UTR. (A) Bioinformatics prediction of miR-92a targeting of human (h) and mouse (m) SIRT1 3'UTR. ΔG is in the unit of kCal/mol and the conserved nucleotides are labeled with asterisk (*). The red box indicates the nucleotide mutated in the luciferase construct used in C. (B, C) HEK-293 cells were transfected with luciferase reporter containing WT SIRT1 3'UTR (B) or its mutant (mut) (C). The cells were co-transfected with control RNA or pre-miR-92a at 20 nM for 72-hour before luciferase activity assay. (D, E) HUVECs were transfected with control RNA or pre-miR-92a as indicated. SIRT1 mRNA level was detected using RT-qPCR (D) and various molecules assessed by IB (E).

Supplemental Figure 3. Vasodilation is impaired in EC-SREBP2(N)-Tg mice. Flow-mediated vasodilation was assessed in carotid arteries from 8- to 10-week-old EC-SREBP2(N) and their wild-type littermates.

Supplemental Figure 4. Systemic administration of LNA-92a inhibits miR-92a targeting and attenuates atherosclerotic lesion in the aortic arch. (A) Total RNA was extracted from thoracic aortas pooled from 4 mice/group (with tail-vein injection of control LNA or LNA-92a) and underwent RT-qPCR. Levels of miR-92a and mRNAs encoding miR-92a targets (SIRT1,

KLF2, and KLF4) were quantified and U6/β-actin was used as respective internal control. (B) Representative *en face* images showing lesion development in the aortic arch of $ApoE^{-/-}$/EC-SREBP2(N) mice fed normal chow and infused with Ang II for 28 days. The age of mice and tail-vein injection of LNA-Ctrl or LNA-92a are as indicated. Bar = 0.5 cm. (C) Quantification of lesion areas in the aortic arches. Student's t test was used to analyze the statistical difference between two groups. * denotes $p < 0.05$ between indicated groups.

Supplemental Figure 5. Ox-PAPC induction of SREBP2. Various proteins were detected by IB in HUVECs treated with ox-PAPC for 12 h at indicated doses (A), treated with ox-PAPC with or without SOD for 12-hour (B), or pretreated with 25-hydroxycholesterol (25-HC) for 12-hour, and then with or without ox-PAPC for 12-hour (C).

Supplemental Figure 6. c-Myc, NF-κB, and TLRs are involved in oxidative stress induction of miR-92a in ECs. HUVECs were transfected with c-Myc siRNA, RelA/p65 siRNA (10 nM) or control RNA, and then stimulated with H_2O_2 (100 μM) for 24-hour (in A) or pretreated with control (Ctrl) or Myd88 inhibitory peptides (Myd88in) (100 μM each) 8-hour prior to stimulation with ox-LDL (50 μg/ml) for 16-hour (in B). The level of miR-92a was detected by Taqman miRNA qPCR, with U6 as the internal control. Data are mean±SEM of 4 independent experiments. * indicates $p < 0.05$ between groups in comparison.

Supplemental Figure 7. Induction of SREBP2 in the aorta of aging mice. SREBP2 mRNA was quantified by RT-qPCR in whole aortas isolated from 3- and 12-month-old C57BL6. n denotes numbers of aortas collected per group.

Supplemental References

1. Matys V, Kel-Margoulis OV, Fricke E, Liebich I, Land S, Barre-Dirrie A, Reuter I, Chekmenev D, Krull M, Hornischer K, Voss N, Stegmaier P, Lewicki-Potapov B, Saxel H, Kel AE and Wingender E. TRANSFAC and its module TRANSCompel: transcriptional gene regulation in eukaryotes. *Nucleic Acids Res*. 2006;34:D108-110.
2. Kel AE, Gossling E, Reuter I, Cheremushkin E, Kel-Margoulis OV and Wingender E. MATCH: A tool for searching transcription factor binding sites in DNA sequences. *Nucleic Acids Res*. 2003;31:3576-3579.
3. John B, Enright AJ, Aravin A, Tuschl T, Sander C and Marks DS. Human MicroRNA targets. *PLoS Biol*. 2004;2:e363.
4. Wu W, Xiao H, Laguna-Fernandez A, Villarreal G, Jr., Wang KC, Geary GG, Zhang Y, Wang WC, Huang HD, Zhou J, Li YS, Chien S, Garcia-Cardena G and Shyy JY. Flow-Dependent Regulation of Kruppel-Like Factor 2 Is Mediated by MicroRNA-92a. *Circulation*. 2011;124:633-641.
5. Fang Y and Davies PF. Site-specific microRNA-92a regulation of Kruppel-like factors 4 and 2 in atherosusceptible endothelium. *Arterioscler Thromb Vasc Biol*. 2012;32:979-987.
6. Fehrenbach ML, Cao G, Williams JT, Finklestein JM and Delisser HM. Isolation of murine lung endothelial cells. *Am J Physiol Lung Cell Mol Physiol*. 2009;296:L1096-1103.
7. Amabile N, Guerin AP, Leroyer A, Mallat Z, Nguyen C, Boddaert J, London GM, Tedgui A and Boulanger CM. Circulating endothelial microparticles are associated with vascular dysfunction in patients with end-stage renal failure. *J Am Soc Nephrol*. 2005;16:3381-3388.

Oxidative Stress Activates Endothelial Innate Immunity via Sterol Regulatory Element Binding Protein 2 (SREBP2) Transactivation of MiRNA-92a

Zhen Chen, Liang Wen, Marcy Martin, Chien-Yi Hsu, Longhou Fang, Feng-Mao Lin, Ting-Yang Lin, McKenna J. Geary, Gregory Geary, Yongli Zhao, David A. Johnson, Jaw-Wen Chen, Shing-Jong Lin, Shu Chien, Hsien-Da Huang, Yury I. Miller, Po-Hsun Huang and John Y-J. Shyy

Circulation. published online December 30, 2014;
Circulation is published by the American Heart Association, 7272 Greenville Avenue, Dallas, TX 75231

Print ISSN: 0009-7322. Online ISSN: 1524-4539